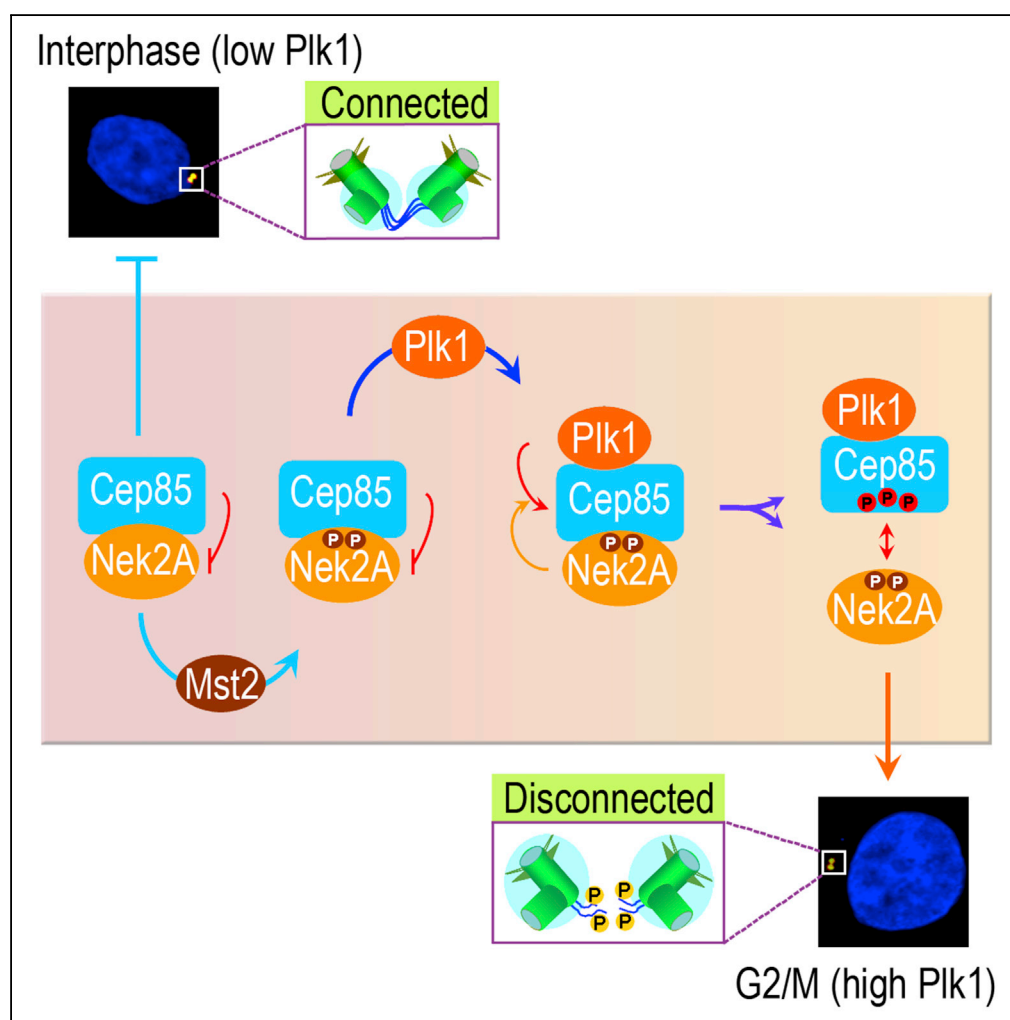


## Article

## Cep85 Relays Plk1 Activity to Phosphorylated Nek2A for Its Timely Activation in Centrosome Disjunction



Canhe Chen,  
Zhenping Xu, Ting  
Zhang, Liping Lin,  
Mingke Lu,  
Changchuan Xie,  
Xianwen Yu

chench@xmu.edu.cn (C.C.)  
yuxw@xmu.edu.cn (X.Y.)

**HIGHLIGHTS**

Cep85 prevents centrosome separation by binding to and inhibiting Nek2A in interphase

Plk1 binds to Cep85 and forms a ternary Plk1-Cep85-Nek2A complex in late G2

Nek2A-assisting Cep85 phosphorylation by Plk1 releases phospho-Nek2A from Cep85

Freed phospho-Nek2A initiates centrosome separation in G2/M

Chen et al., iScience 11, 114–133  
January 25, 2019 © 2018 The Author(s).  
<https://doi.org/10.1016/j.isci.2018.12.013>

## Article

# Cep85 Relays Plk1 Activity to Phosphorylated Nek2A for Its Timely Activation in Centrosome Disjunction

Canhe Chen,<sup>1,\*</sup> Zhenping Xu,<sup>1</sup> Ting Zhang,<sup>1</sup> Liping Lin,<sup>1</sup> Mingke Lu,<sup>1</sup> Changchuan Xie,<sup>1</sup> and Xianwen Yu<sup>1,2,\*</sup>

## SUMMARY

**Timely centrosome separation is critical for accurate chromosome separation. It is initiated by Nek2A at the onset of mitosis, but the mechanism for the strict requirement of phosphorylated Nek2A for its own activation remains unclear. In this study, we have found that Plk1 interacts with Cep85 and forms a ternary complex with Cep85-Nek2A. Nek2A binding, but not its kinase activity, is pre-required for Cep85 to be phosphorylated by Plk1. Nek2A-dependent Cep85 phosphorylation, in turn, leads to the dissociation of phosphorylated Cep85 exclusively from phospho-Nek2A, thereby increasing the freed phospho-Nek2A activity. Both kinases are also required for phosphorylating endogenous Cep85 in cells, and timely phosphorylation of Cep85 and Nek2A is crucial for initiating centrosome disjunction at G2/M. Overall, our study has uncovered a previously unrecognized role of Plk1 and Nek2A and identified Cep85 as a missing piece directly relaying Plk1 activity to Nek2A for its activation in centrosome disjunction.**

## INTRODUCTION

The centrosomes are crucial for bipolar spindle formation in human cells. They are composed of the centrioles acting as a core and the surrounding pericentriolar materials from which microtubules are nucleated and organized (Bornens, 2012; Nigg and Raff, 2009). As cells pass through mitosis, the two tightly associated centrioles in one centrosome are disengaged to form two separated centrioles (Avidor-Reiss and Gopalakrishnan, 2013; Azimzadeh and Bornens, 2007; Bettencourt-Dias and Glover, 2007). They are held together through a proteinaceous linker consisting of a number of proteins, such as rootletin, Cep68, LRRC45, and C-Nap1 (Bahe et al., 2005; Fry et al., 1998a; Graser et al., 2007; He et al., 2013). C-Nap1 is a large coiled-coil protein locating at the proximal end of centrioles and acting as a docking site for the linker proteins such as rootletin and LRRC45 (He et al., 2013; Yang et al., 2006). This linker persists from G1 till late G2, when it is disassembled and the two linked centrosomes are subsequently disconnected and pulled apart to the opposite poles of the cell by the motor proteins, such as Eg5, for spindle formation in mitosis (Mardin et al., 2010; Mardin and Schiebel, 2012).

At the onset of mitosis, NIMA (never in mitosis A)-related kinase Nek2A is the primary kinase responsible for initiating centrosome separation (also called centrosome disjunction) (Mardin and Schiebel, 2012; van Ree et al., 2016; Wang et al., 2014). It phosphorylates C-Nap1, rootletin, and LRRC45, thereby disassembling the linker to disconnect the centrosomes (Bahe et al., 2005; Faragher and Fry, 2003; Fry et al., 1998a; Hardy et al., 2014; He et al., 2013). Nek2A itself is also subject to phosphorylation by a hippo pathway component Mst2 at four serine residues including Ser356, Ser365, Ser406, and Ser438 in its non-catalytic C-terminal region (Mardin et al., 2010). This in turn accelerates phosphorylated Nek2A to further accumulate at centrosomes. Preventing phosphorylation at these residues by Ala replacement leads to Nek2A incapability to induce premature centrosome separation (also called centrosome splitting) (Mardin et al., 2010, 2011). Given that the unphosphorylated Nek2A is still able to accumulate at centrosomes, albeit the level being slightly reduced in some cases (Mardin et al., 2010, 2011), the precise mechanism underlying its incapability to induce centrosome splitting remains uncertain. Nevertheless, the accumulation of phosphorylated, but not unphosphorylated, Nek2A at centrosomes appears to be necessary for centrosome disjunction.

In G2, besides Nek2A, three other mitotic kinases including Cdk1, Plk1, and Aurora A (AurA) are also implicated in centrosome disjunction (Mardin et al., 2011; Mardin and Schiebel, 2012; van Ree et al., 2016; Wang et al., 2014). Among them, AurA is mainly responsible for the activation of Plk1 by phosphorylating Thr210 residue in the activation loop of Plk1 (Macurek et al., 2008; Seki et al., 2008). In this process, binding of

<sup>1</sup>State Key Laboratory of Cellular Stress Biology, School of Life Sciences, Xiamen University, Xiamen, Fujian 361102, China

<sup>2</sup>Lead Contact

\*Correspondence: chench@xmu.edu.cn (C.C.), yuxw@xmu.edu.cn (X.Y.)

<https://doi.org/10.1016/j.isci.2018.12.013>



CDK1-dependent phosphorylated Bora to Plk1 is pre-required for AurA to access the activation loop (Parrilla et al., 2016). Plk1 is a serine/threonine kinase that is crucial for centrosome maturation, spindle assembly, microtubule-kinetochore attachment, and cytokinesis (Bruinsma et al., 2012). It localizes at centrosomes and plays pivotal roles in centrosome disjunction at the onset of mitosis by activating Nek2A as well as motor protein Eg5 (Mardin et al., 2011; Smith et al., 2011). Mst2 is one of its centrosomal targets that is implicated in regulating Nek2A activity. Plk1-dependent phosphorylation of Mst2 at three residues including Ser15, Ser18, and Ser316 locating outside its kinase domain leads to the dissociation of protein phosphatase 1 gamma (PP1 $\gamma$ ) from Mst2-Nek2A-PP1 $\gamma$  complex, thereby preventing PP1 $\gamma$  from further dephosphorylating C-Nap1 (Mardin et al., 2011). Given that PP1 $\gamma$  does not directly dephosphorylate Nek2A (Mardin et al., 2011), and that it has never been detected to localize at centrosomes where Nek2A resides, it is unknown to what extent Plk1 actually contributes to Nek2A activation through this process. The facts that inhibition or depletion of Plk1 leads to cell cycle arrest in a prometaphase-like state with unseparated centrosomes (Liu and Erikson, 2002; Mardin et al., 2011), and that it is recruited to centrosomes during S, G2, and mitosis and is first activated in G2 (Macurek et al., 2008; Seki et al., 2008), indicate that Plk1 should play some unidentified roles critical for determining Nek2A activation at centrosomes in late G2.

Recently, we have identified a centrosomal protein Cep85 as another negative regulator for Nek2A (Chen et al., 2015). It can physically interact with and suppress Nek2A kinase activity. The Nek2A-binding domain (NBD), a region within Cep85, has been defined to interact with the non-catalytic C-terminal region of Nek2A (Chen et al., 2015), where four residues that have been identified to be phosphorylated by Mst2 and are essential for Nek2A activation in late G2 reside (Mardin et al., 2010). However, the exact mechanism of Nek2A inhibition upon Cep85 binding to its noncatalytic region remains unknown. Importantly, Cep85 co-localizes with Nek2A at the proximal end of centrosomes and also steadily increases its level at centrosomes from G1 to G2. Cep85 depletion leads to centrosome splitting, and overexpression can overcome the effect of Nek2A overexpression, which would otherwise lead to centrosome splitting. Given that it appears at the right time and right place, and acts in the right way, we propose that Cep85 is the primary negative regulator at centrosomes to antagonize Nek2A to maintain the centrosomal integrity in interphase. If it is the case, there should exist a substantial way for Nek2A to overcome Cep85 antagonism to elevate its kinase activity for centrosome disjunction at G2/M transition.

In this study, we have employed a number of biochemical and biological strategies to address the mechanism of Cep85 regulation in late G2 and have revealed a critical role for Plk1 and Nek2A at centrosomes for centrosome disjunction.

## RESULTS

### Plk1 Interacts with Cep85

To date, it is unclear how Nek2A activity at centrosomes can achieve a threshold level in the presence of a large amount of its antagonist Cep85 at the onset of mitosis. Based on our previous findings showing that Nek2A once co-expressed with Cep85 can induce Cep85 phosphorylation (Chen et al., 2015), we reasoned that Cep85 phosphorylation might affect Cep85-Nek2A affinity. Given that Nek2A is not the kinase directly phosphorylating Cep85 (Chen et al., 2015), we decided to identify the potential kinase. We first co-expressed Cep85 with five kinases that are required for centrosome disjunction including AurA, Cdk1, Mst2, Nek2A, and Plk1, individually, and examined the mobility shift of Cep85. Compared with the control, co-expression of AurA did not lead to the mobility shift of Cep85, Cdk1 displayed a negligible effect, Mst2 exhibited a moderate effect, and Plk1 had a significant effect similar to Nek2A (Figure 1A). Meanwhile, Cep85 could co-immunoprecipitate with AurA, Cdk1, Plk1, and Nek2, which has been reported previously (Chen et al., 2015). Among them, Plk1 exhibited the highest affinity to Cep85 (Figure 1B). As Plk1 can strongly bind to and cause a mobility shift of Cep85, we further investigated their interaction in detail. Reciprocal co-immunoprecipitation revealed that Cep85 was also complexed with immunoprecipitated Plk1 (Figure 1C). In addition, the endogenous Plk1 could be co-immunoprecipitated by the endogenous Cep85 (Figure 1D). The physical interaction between Cep85 and Plk1 was further confirmed by the reciprocal co-immunoprecipitation of the endogenous proteins (Figure 1E). Furthermore, *in vitro* GST pull-down assays revealed that insect-cell-produced Plk1 could bind to the recombinant Cep85 protein (Figure 1F). Consistent with previous reports (Macurek et al., 2008; Seki et al., 2008), quantitative image analyses revealed that Plk1 first appeared at centrosomes with a low level around early G2 and was steadily increased thereafter (Figures 1G and 1I). When co-stained with Cep85, Plk1 was readily detected to partially

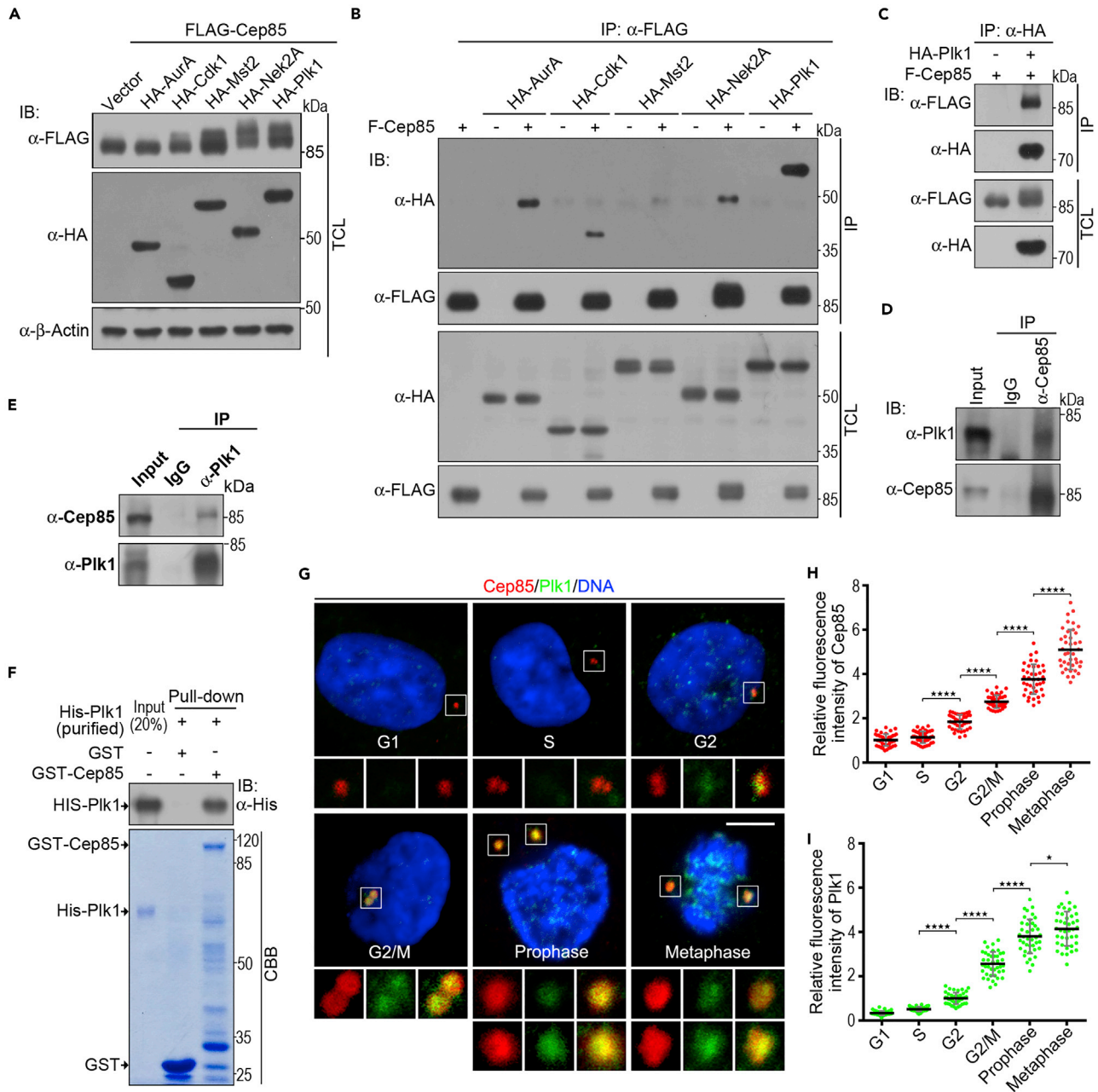


**Figure 1. Plk1 Interacts with Cep85**

(A–C) HEK293T cells were co-transfected with FLAG-Cep85 and hemagglutinin (HA)-tagged kinases. The cell lysates were subjected to immunoblotting (IB) assays to detect the mobility shift of Cep85 (A), or to co-immunoprecipitation assays followed by immunoblotting, to determine the binding affinity of the indicated kinases to Cep85 (B) and the binding affinity of Cep85 to Plk1 (C). TCL, total cell lysates; IP, immunoprecipitation.

(D) The endogenous Cep85 was precipitated (IP) from HEK293T cell lysates with anti-Cep85 antibody, and anti-Plk1 antibody was used to detect Plk1 in the precipitates and cell lysates (Input).

(E) The endogenous Plk1 was precipitated (IP) from HEK293T cell lysates with anti-Plk1 antibody, and anti-Cep85 antibody was used to detect Cep85 in the precipitates and cell lysates (Input).

(F) The interaction of the bacterially produced GST-Cep85 and His-tagged Plk1 purified from insect cells was examined by *in vitro* GST pull-down assays. CBB, Coomassie brilliant blue stain.

(G–I) The cell-cycle-dependent co-localization of Cep85 and Plk1 in HeLa cells were revealed by co-immunostaining with anti-Cep85 (red) and anti-Plk1 (green) antibodies. DNA (blue) was stained with DAPI (G). The boxed areas are shown at a higher magnification directly below the corresponding image. Scale bar, 5  $\mu$ m. The relative fluorescent intensities of Cep85 and Plk1 from 40 cells in individual stages were quantitated and plotted in (H) and (I), respectively. \* $p < 0.05$ , \*\*\*\* $p < 0.0001$ .

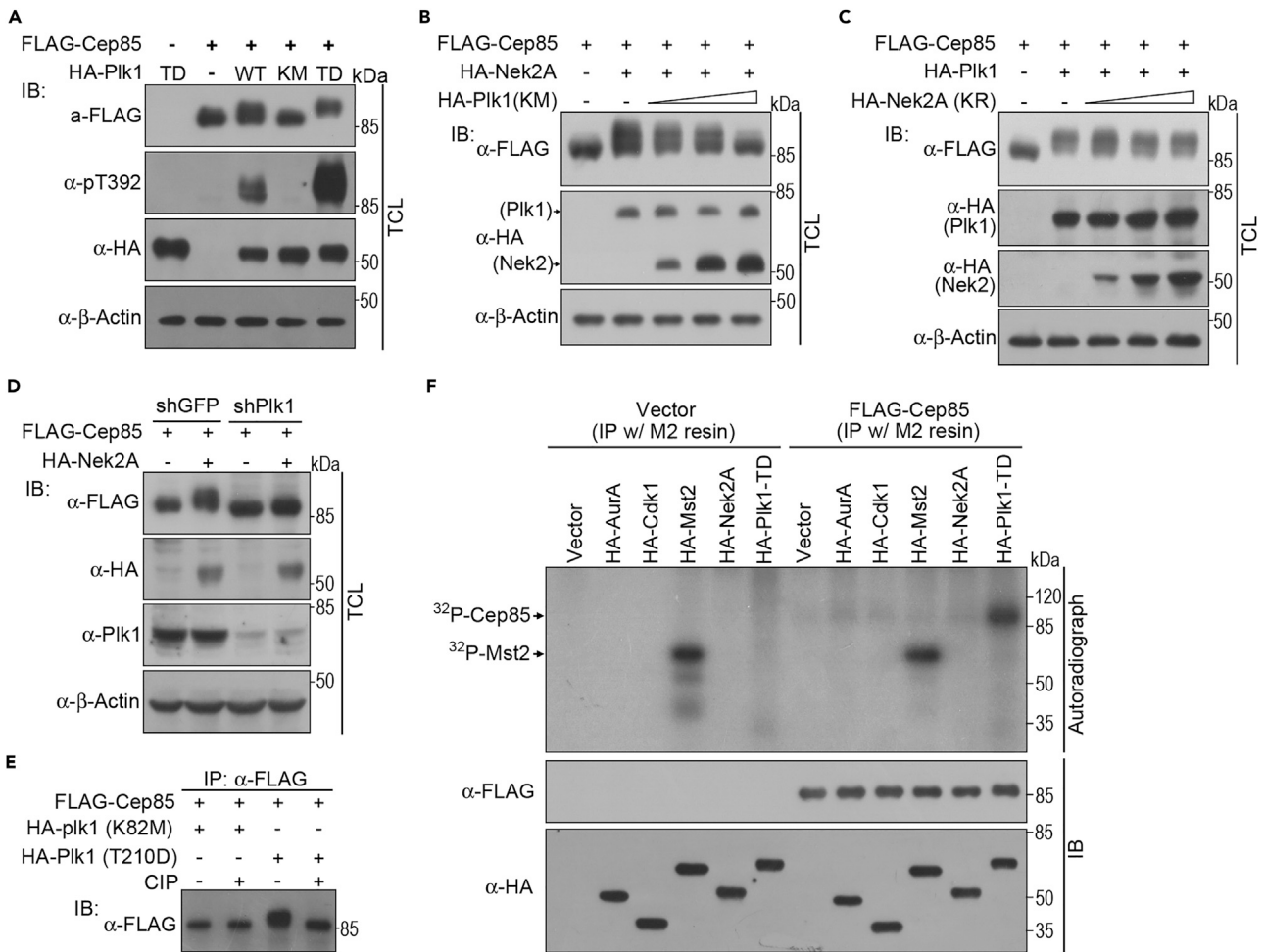


**Figure 2. Plk1 Is the Genuine Kinase to Phosphorylate Cep85**

(A) The differential effects of Plk1 proteins on Cep85 mobility shift. FLAG-Cep85 was co-expressed with indicated Plk1 constructs in HEK293T cells, individually. Cep85 phosphorylation was displayed by immunoblotting (IB) to reveal its mobility shift with anti-FLAG antibody and its phosphorylation of Cep85-Thr392 with phospho-antibody anti-pT392 (referring to Figure 3). TCL, total cell lysates; WT, wild-type; KM, kinase-dead mutant Plk1-K82M; TD, constitutively active mutant Plk1-T210D.

(B) Different amounts of kinase-dead mutant HA-Plk1-K82M were co-expressed with FLAG-Cep85 and HA-Nek2A in HEK293T cells. The mobility shift of FLAG-Cep85 was visualized by western blot.

(C) Different amounts of the kinase-dead mutant HA-Nek2A-K37R were co-expressed with FLAG-Cep85 and wild-type HA-Plk1 in HEK293T cells. The mobility shift of FLAG-Cep85 was visualized by western blot.

(D) HEK293T cells were infected with indicated lentiviral shRNAs 12 hr before co-transfection with FLAG-Cep85 and HA-Nek2A. Cell lysates were prepared 20 hr post-transfection and subjected to immunoblotting.

(E) FLAG-Cep85 co-transfected either with active Plk1-T210D or inactive Plk1-K82M in HEK293T cells was immunoprecipitated and subjected to the calf-intestinal alkaline phosphatase (CIP) treatment analysis.

(F) FLAG-Cep85 and HA-tagged kinases were immunoprecipitated from HEK293T cell lysates, individually, and subjected to *in vitro* kinase assay with [ $\gamma$ - $^{32}$ P]-ATP. The phosphorylated proteins were detected by autoradiography.

co-localize with Cep85 in early G2, increasingly at G2/M, and extensively from prophase to metaphase (Figures 1G–1I). These results reveal that Plk1 physically interacts with Cep85 at centrosomes, suggesting that Plk1 could be the kinase phosphorylating Cep85.

**Plk1 Is the Genuine Kinase to Phosphorylate Cep85**

To verify whether Plk1 is the real kinase phosphorylating Cep85, we first utilized a kinase-dead mutant Plk1-K82M to examine whether this dominant negative mutant could block Nek2A-induced Cep85 mobility shift. Plk1-K82M was confirmed to have lost its capability to phosphorylate Cep85 (Figure 2A). It could

gradually decrease the mobility shift of Cep85 induced by Nek2A in a dosage-dependent manner (Figure 2B). Conversely, a kinase-dead mutant Nek2A-K37R could not prevent the mobility shift of Cep85 induced by Plk1 even at a high dosage (Figure 2C). These results thus suggest that Plk1 might act downstream of Nek2A and be the candidate kinase responsible for Nek2A-induced Cep85 phosphorylation. This is further supported by the finding showing that Nek2A-induced Cep85 mobility shift could be suppressed by short hairpin RNA (shRNA)-mediated depletion of the endogenous Plk1 (Figure 2D). Furthermore, the calf-intestinal alkaline phosphatase treatment assays revealed that the kinase for Cep85 phosphorylation is a serine/threonine kinase (Figure 2E). To directly demonstrate that Plk1 is the real kinase to phosphorylate Cep85, we performed *in vitro* kinase assays. Among five kinases, only Plk1 could efficiently phosphorylate Cep85 that was expressed in mammalian cells, whereas Mst2 could itself be autophosphorylated (Figure 2F). We thus conclude that Plk1 is the genuine kinase responsible for Cep85 mobility shift induced by Nek2A in cells, an issue that was raised in our previous report but remained unsolved (Chen et al., 2015).

### Plk1 Heavily Phosphorylates the Nek2A-Binding Domain in Cep85 at Centrosomes in Late G2

To address whether Cep85 phosphorylation could affect Cep85-Nek2A affinity, we decided to identify the phospho-sites in Cep85 first. We initially applied a full-length Cep85 that had been co-expressed with wild-type Plk1 to mass spectrometry. Over 30 serine/threonine residues in Cep85 were identified to be phosphorylated across the whole sequence, but few sites were located in the NBD (amino acid [aa] 257–433) defined previously (Chen et al., 2015) (data not shown). This prompted us to modify our approaches for sample preparation by using N-terminal truncated Cep85 (aa 1–543) and a constitutively active mutant Plk1-T210D (Figure S1A). Six residues within the NBD including Ser280, Ser352, Ser361, Thr392, Ser406, and Ser417 were identified to be phosphorylated (Figure S1B, highlighted in red). Among them, a phosphopeptide with the amino acid sequence QREN-pT-FLRAQFAQK around Thr392 was chosen as an antigen for the phospho-specific antibody production.

The produced phospho-antibody against phospho-Thr392 in Cep85 (hereafter referred to as anti-pT392) was first subjected to analysis for its specificity. This phospho-antibody could specifically recognize the Cep85 protein that was co-expressed with Plk1-wild-type (WT) or Plk1-T210D, but not with Plk1-K82M (Figure 2A). It also could not recognize Cep85-T392A in which Thr392 had been altered to Ala (Figure 3A). Furthermore, this antibody could recognize a protein at centrosomes with a low signal in G2 but a strong signal in M (Figures 3B–3D, shGFP). This signal completely disappeared in G2 and remarkably reduced in M after Cep85 was depleted (Figures 3B–3D, shCep85). The remnant signal in M was likely due to the low levels of Cep85 at centrosomes (Figures S2A–S2D). All together, these results validate that our anti-pT392 antibody can specifically recognize the phosphorylated Cep85 induced by Plk1. It is noteworthy that Cep85 depletion undoubtedly led to centrosome splitting (Figures 3B and S2A). This is consistent with our previous report and emphasizes the importance of Cep85 in maintaining centrosome integrity in interphase (Chen et al., 2015).

Next, we examined Cep85 phosphorylation throughout the cell cycle in detail. Consistent with our previous findings (Chen et al., 2015), we observed that Cep85 resided at centrosomes throughout the whole cell cycle and steadily increased its levels from G1 to M phase (Figures 3E and 3F). In comparison, phosphorylated Cep85 could be detected barely in early G2 but readily at G2/M with a steeply increased level; it reached the maximal level in metaphase (Figures 3E and 3G). The intensity of Cep85 phosphorylation was increased over 2.5-fold at G2/M and approximately 4-fold in metaphase compared with that in G2 (Figure 3G). These results revealed that Cep85 is heavily phosphorylated at centrosomes at G2/M.

The pattern of Cep85 phosphorylation shown above is reminiscent of the activity of Plk1 over the cell cycle (Macurek et al., 2008; Seki et al., 2008). To validate the relationship between Cep85 phosphorylation and Plk1 activity, we synchronized HeLa cells and examined Cep85 phosphorylation over the cell cycle by western blot. The expression patterns of Nek2A and Cyclin B1 validated the synchrony of cell cycle (Figure 3H). Remarkably, our anti-pT392 phospho-antibody could also recognize the endogenous Cep85 protein detected by immunoblotting (Figure 3H). The overt Cep85 phosphorylation appeared at 8.5 hr, was increased at 9 and 10 hr, and was greatly reduced at 11 hr onward, whereas Cep85 protein remained unchanged throughout the cell cycle. Plk1 protein was steadily increased from 6 to 10 hr, slightly reduced at 11 hr, and steeply decreased to a basal level thereafter. Its activity, revealed by anti-Plk1pT210, remained

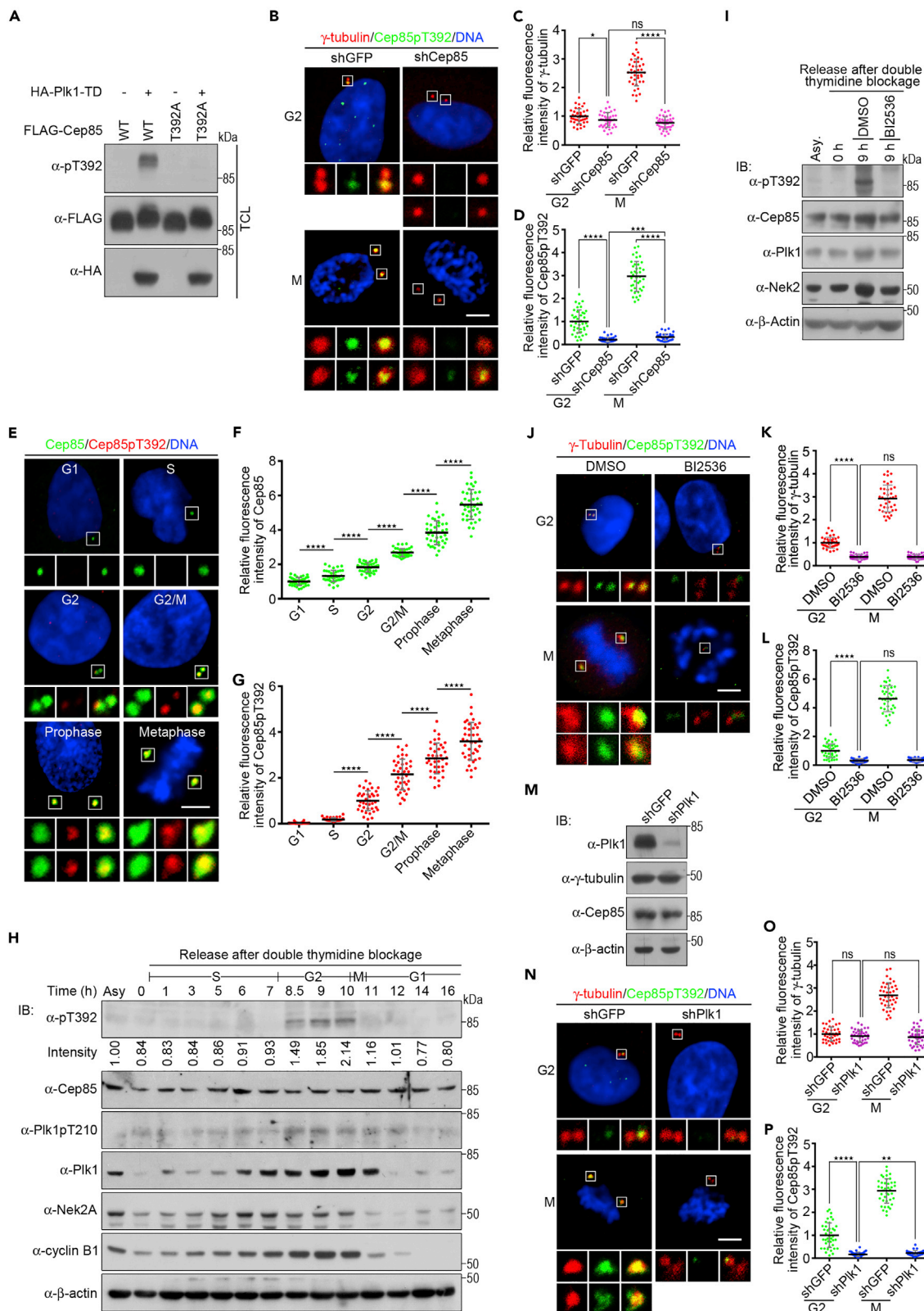


**Figure 3. Plk1 Is Required for Cep85 Phosphorylation**

(A–D) Validation of the specificity of phospho-antibody anti-pT392. WT and T392A mutant of FLAG-Cep85 were co-expressed with active mutant Plk1-T210D (Plk1-TD) in HEK293T cells. Western blot was employed to detect the phosphorylation of Thr392 residue in Cep85 with anti-pT392 antibody as well as the mobility shift of Cep85 proteins with anti-FLAG antibody (A). (B) HeLa cells were infected with either shGFP (control) or shCep85 lentiviral particles 72 hr before co-immunostaining with anti- $\gamma$ -tubulin (red) and anti-pT392 (green). The relative fluorescent intensities of  $\gamma$ -tubulin and Cep85pT392 were quantitated and plotted in (C) and (D), respectively. HA, hemagglutinin.

(E–G) (E) HeLa cells were fixed and stained with anti-Cep85 antibody for endogenous Cep85 (green) and with anti-pT392 for phosphorylated Cep85 (red). The relative fluorescent intensities of Cep85 and Cep85pT392 were quantitated and plotted in (F) and (G), respectively.

(H) HeLa cells were enriched at G1/S using a double thymidine block. After releasing, cells were harvested at indicated time points before western blot analysis with antibodies to detect the endogenous proteins, individually. The levels of Cep85 phosphorylation from one representative experiment were quantitated and shown directly below the western blot with anti-pT392 antibody.

(I–L) HeLa cells were synchronized using a double thymidine block. After releasing, cells were further treated either with DMSO (control) or BI2536. They were either harvested at 9 hr post-treatment before immunoblotting (IB) with indicated antibodies to detect phosphorylated Cep85 as well as the endogenous proteins, individually (I), or fixed at 8 hr and 11 hr post-treatment before co-immunostaining with anti- $\gamma$ -tubulin (red) and anti-pT392 (green) (J). The relative fluorescent intensities of  $\gamma$ -tubulin and Cep85pT392 in (J) were quantitated and plotted in (K) and (L), respectively.

(M–P) HeLa cells were infected with the indicated lentiviral shRNAs 20 hr before either western blot analysis (M) or fixation for co-immunostaining with antibodies against  $\gamma$ -tubulin (red) and phospho-Thr392 (green) in (N). The relative fluorescent intensities of  $\gamma$ -tubulin and Cep85pT392 were quantitated and plotted in (O) and (P), respectively. For immunostaining experiments, the boxed areas are shown at a higher magnification directly below the corresponding image. The relative fluorescent intensities of the indicated proteins from 40 cells in each group were quantified. Data are mean  $\pm$  SEM; ns, not significant; \* $p < 0.05$ ; \*\* $p < 0.01$ ; \*\*\* $p < 0.001$ ; \*\*\*\* $p < 0.0001$ . Scale bar, 5  $\mu$ m. See also [Figures S1 and S2](#).

high from 8.5 to 11 hr ([Figure 3H](#)). These results indicate that the levels of Cep85 phosphorylation are well correlated with Plk1 activity over the cell cycle.

To further confirm that Plk1 phosphorylates Cep85 *in vivo*, we utilized BI2536 to inhibit Plk1 activity or the shRNA technique to deplete Plk1 in cells before examining the effect of Plk1 inhibition/depletion on Cep85 phosphorylation. Consistent with the above findings ([Figure 3H](#)), Cep85 was heavily phosphorylated at 9 hr after releasing from a double thymidine block ([Figure 3I](#), DMSO). It, however, was no longer phosphorylated after BI2536 treatment ([Figure 3I](#), BI2536). The effect of Plk1 inhibition on Cep85 phosphorylation was alternatively confirmed by immunostaining with anti-pT392 antibody after BI2536 treatment, revealing a dramatic decrease of Cep85 phosphorylation and  $\gamma$ -tubulin accumulation at centrosomes ([Figures 3J and 3K](#)). Similar to Plk1 inhibition above, Plk1 depletion also resulted in a significant reduction of Cep85 phosphorylation ([Figures 3N–3P](#)), although it did not alter the overall levels of Cep85 or  $\gamma$ -tubulin ([Figure 3M](#)). These results further confirm that Plk1 is the genuine kinase phosphorylating endogenous Cep85 in cells.

**Nek2A Binding but Not Its Kinase Activity Is Pre-required for Cep85 to be Phosphorylated by Plk1**

Given that Nek2A cannot phosphorylate Cep85 and Plk1 is the real kinase phosphorylating Cep85 ([Figures 2 and 3](#)), it seemed that Nek2A might not be required for Plk1-mediated Cep85 phosphorylation. However, it is not the case. When the endogenous Nek2A was depleted, Plk1 could no longer phosphorylate Cep85 ([Figure 4A](#)), the endogenous Cep85 protein that was heavily phosphorylated in late G2 was not phosphorylated any more ([Figure 4B](#), 9 hr), and phosphorylated Cep85 at centrosomes was lost in G2 and substantially reduced in M ([Figures 4C–4E](#)). In contrast, Nek2A depletion did not alter the overall level of Cep85 or  $\gamma$ -tubulin ([Figure S3](#)). Unlike Plk1 inhibition or depletion, Nek2A depletion had less effect on centrosomal integrity, judged by the higher levels of  $\gamma$ -tubulin retained at centrosomes in the Nek2A-depleted cells ([Figures 4C and 4D](#)) than in the Plk1-inhibited or Plk1-depleted cells ([Figures 3J, 3K, 3N, and 3O](#)).

To find out the mechanism by which Nek2A is required for Cep85 phosphorylation, we carried out *in vitro* kinase assays by using bacterially produced GST-Cep85 instead of mammalian-cell-expressed Cep85, which had been shown to be an excellent substrate for Plk1 ([Figure 2F](#)). To our surprise, GST-Cep85 could not be phosphorylated by any kinases, whereas the autophosphorylation of Mst2 kinase was again readily detected ([Figure 4F](#)). We reasoned that something was missing from bacterially produced GST-Cep85. It is indeed the case. After pre-incubating GST-Cep85 with FLAG-Nek2A to form a Cep85-Nek2A complex, Plk1 again could phosphorylate GST-Cep85 ([Figure 4G](#)). Remarkably, phosphorylated GST-Cep85 could be readily recognized due to a prominent mobility shift after prolonged separation (p.s.) of the samples in SDS-PAGE ([Figure 4G](#), CBB p.s.). Importantly, this provides us a simpler approach to examine Cep85 phosphorylation than autoradiography *in vitro*.

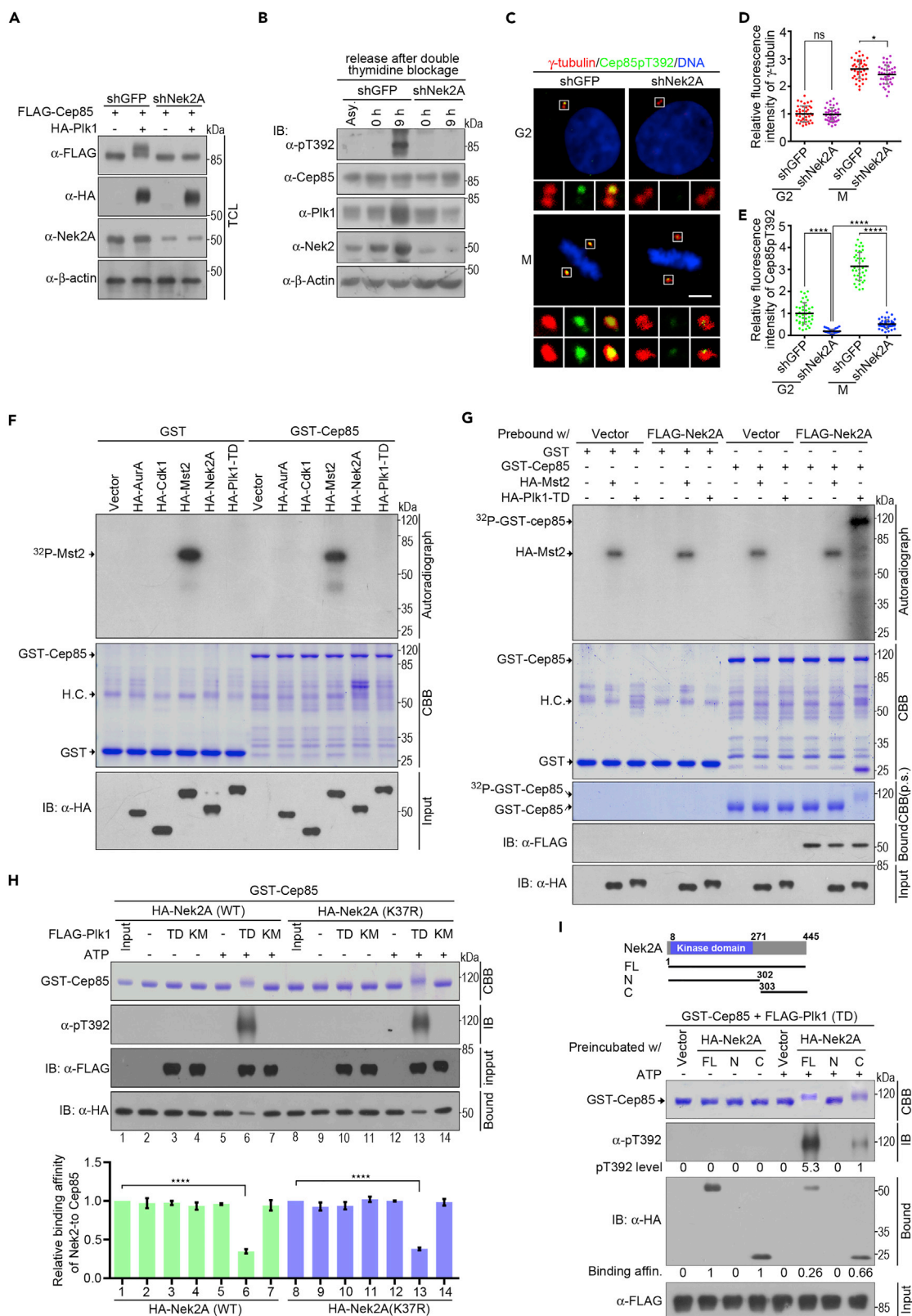


#### Figure 4. Nek2A Binding, but Not Its Kinase Activity, Is Pre-required for Cep85 Phosphorylation by Plk1

(A) HEK293T cells were infected with indicated lentiviral shRNAs for 30 hr before co-transfection with FLAG-Cep85 and HA-Plk1. Cell lysates were prepared and subjected to immunoblotting 20 hr post-transfection. HA, hemagglutinin.

(B) HeLa cells were infected with indicated lentiviral shRNAs 20 hr before synchronization with a double thymidine block. After releasing, cells were harvested at indicated time points followed by immunoblotting (IB) with indicated antibodies.

(C–E) HeLa cells were infected with indicated lentiviral shRNAs for 36 hr before fixation for co-immunostaining with antibodies against  $\gamma$ -tubulin (red) and phosphorylated Cep85-Thr392 (green) (C). The boxed areas in (C) are shown at a higher magnification directly below the corresponding image. The relative fluorescent intensities of  $\gamma$ -tubulin and Cep85pT392 were quantitated and plotted in (D) and (E), respectively. In each group 40 cells were quantified. Data are mean  $\pm$  SEM; ns, not significant; \* $p < 0.05$ ; \*\*\*\* $p < 0.0001$ ; scale bar, 5  $\mu$ m.

(F) The recombinant GST-Cep85 and immunoprecipitated kinases were subjected to *in vitro* kinase assays with [ $\gamma$ -<sup>32</sup>P]-ATP. CBB, Coomassie brilliant blue stain; IB, immunoblotting.

(G) The recombinant GST-Cep85 was incubated with HEK293T cell lysates transfected with indicated constructs before *in vitro* kinase assays with [ $\gamma$ -<sup>32</sup>P]-ATP. The mobility shift of Cep85 was visualized by CBB staining after prolonged separation (p.s.) of samples on an SDS-PAGE.

(H) GST-Cep85 was pre-bound with either active Nek2A-WT or kinase-dead Nek2A-K37R before *in vitro* kinase assays in the presence of either active Plk1-T210D (Plk1-TD) or inactive Plk1-K83M (Plk1-KM). After reaction, the samples were washed to remove unbound proteins before immunoblotting. Prolonged separation followed by CBB staining or western blot with anti-pT392 antibody was used to reveal phosphorylated Cep85. Western blot with anti-HA antibody was applied to detected Nek2A proteins remaining on Cep85 after the kinase reaction. The amount of retained Nek2A was quantitated and plotted in the lower panel. Data are mean  $\pm$  SEM from three independent experiments, \*\*\*\* $p < 0.0001$ .

(I) Schematic diagram of Nek2A deletion mutants are shown in the upper panel. GST-Cep85 was preincubated with cell lysates containing WT, N terminus (N), or C terminus (C) of Nek2A before *in vitro* kinase assays, followed by similar treatments as mentioned in (H). The intensity of Cep85pT392 and the amount of Nek2A proteins that remained on GST-Cep85 were quantitated and are shown below the representative western blots, respectively.

See also [Figures S3](#) and [S4](#).

To determine the contribution of Nek2A kinase activity to Cep85 phosphorylation, we applied additional kinase-dead mutants including Nek2A-K37R and Plk1-K82M to the same assays. As expected, Plk1-T210D could efficiently phosphorylate GST-Cep85 complexing with wild-type Nek2A, judged by the overt mobility shift of GST-Cep85 and immunoblotting with anti-pT392 antibody ([Figure 4H](#), lane 6). Intriguingly, kinase-dead mutant Nek2A-K37R was still able to promote Cep85 phosphorylation to an almost same level, indicating that binding, but not kinase activity, of Nek2A is pre-required for Cep85 to be phosphorylated by Plk1 ([Figure 4H](#), lane 13). In contrast, Plk1-K82M could not phosphorylate Cep85 even in the presence of Nek2A-WT ([Figure 4H](#), lanes 7 and 14), indicating that Plk1 kinase activity is necessary. To determine the amount of Nek2A that remained on Cep85 after it was phosphorylated by Plk1, we had modified the *in vitro* kinase assays by incorporating an additional wash step to remove unbound proteins before denaturing the samples. Importantly, we found that the amount of Nek2A that remained on Cep85 was greatly reduced and that less than 40% of either wild-type or mutant Nek2A was retained on Cep85 ([Figure 4H](#), lanes 6 and 13), indicating that Cep85 phosphorylation may diminish the binding affinity of phospho-Cep85 to Nek2A that was expressed in mammalian cells.

Our previous study has demonstrated that Nek2A binds to Cep85 via its C-terminal region, but not its N-terminal region containing the kinase domain ([Chen et al., 2015](#)). To further confirm that Nek2A binding, but not its kinase activity, is critical for Cep85 phosphorylation, we decided to determine whether binding of the C-terminal region of Nek2A is sufficient for Cep85 phosphorylation. *In vitro* GST pull-down assays confirmed that GST-Cep85 could bind to full-length and C-terminal region of Nek2A ([Figure S4](#)). *In vitro* kinase assays revealed that the C-terminal region of Nek2A could still boost Cep85 phosphorylation, albeit at a less efficiency than the full-length one, but the N-terminal region could not promote Cep85 phosphorylation, which was likely due to its incapability to interact with Cep85 ([Figures 4I](#) and [S4](#)). Consistently, the binding affinity of phosphorylated Cep85 to either full-length or C-terminal Nek2A was significantly reduced and appeared to be inversely proportional to the degree of Cep85 phosphorylation ([Figure 4I](#)). All together, these results reveal that binding, but not the kinase activity, of Nek2A is pre-required for Cep85 to be phosphorylated by Plk1.

#### Binding of Plk1 to Cep85 Does Not Preclude Nek2A from Cep85-Nek2A Complex, and They Can Further Form a Ternary Plk1-Cep85-Nek2A Complex

As both Nek2A and Plk1 can bind to Cep85, we initially hypothesized that there might exist certain types of competition that would eventually lead to the dissociation of Nek2A-Cep85. To test this possibility, we first would like to fine-map the region in Cep85 binding to Plk1. A series of Myc-tagged Cep85 truncated mutants were generated and were co-expressed with HA-Plk1 in HEK293T cells, and co-immunoprecipitation assays were performed ([Figure 5A](#)). We observed that the first 33 aas in Cep85 were not required for Plk1 binding, but that further truncated mutants from the N terminus including M2-5 gradually decreased their

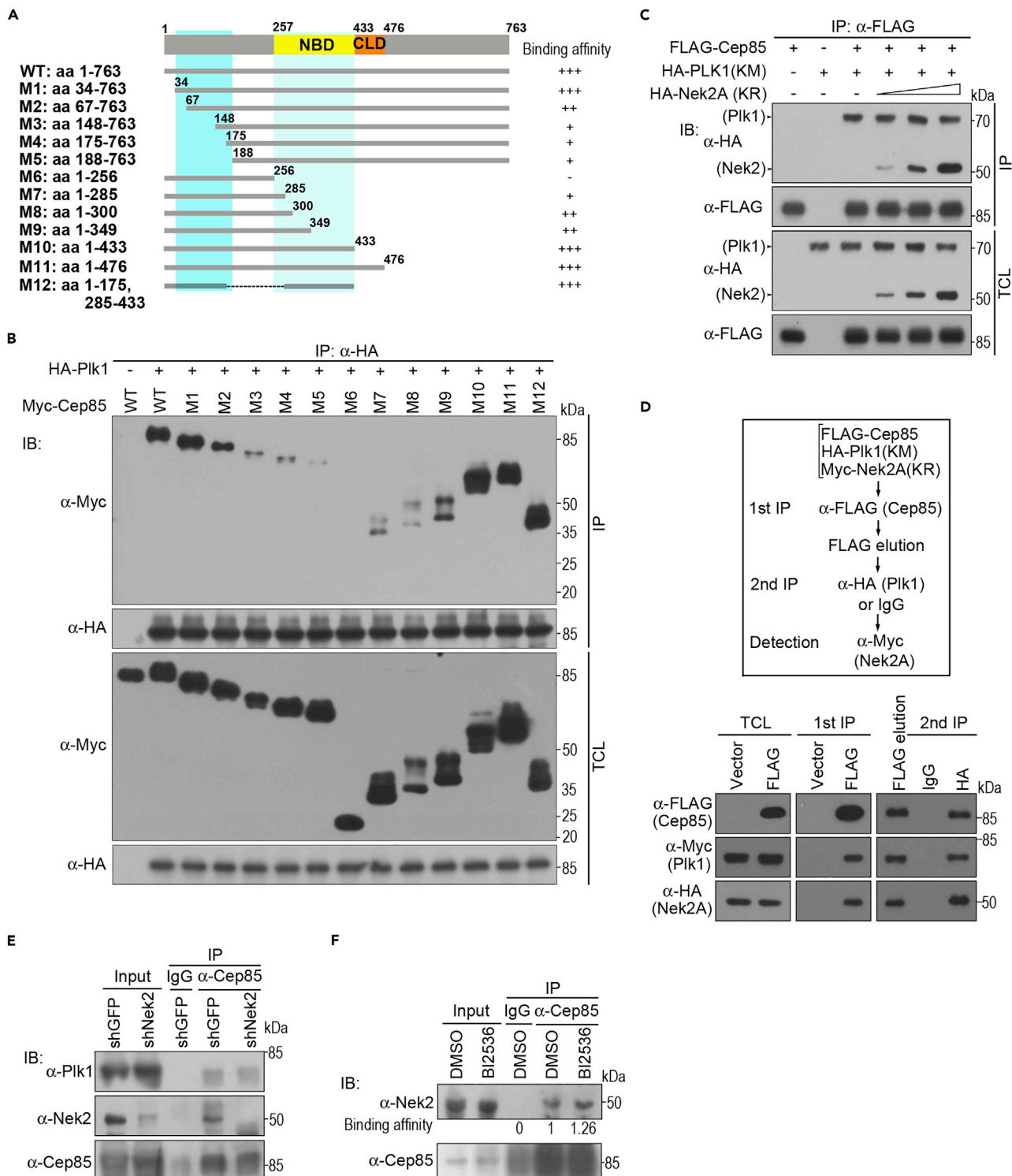


**Figure 5. Binding of Plk1 to Cep85 Does Not Preclude Nek2A from Cep85-Nek2A Complex, and They Can Form a Ternary Plk1-Cep85-Nek2A Complex**

(A and B) Plk1 simultaneously interacts with two small regions in the N-terminal region of Cep85. A schematic diagram of Cep85 and its truncated mutants are shown in (A). The numbers indicate the positions of the first or the last amino acid of individual fragments. The relative binding affinity of the truncated mutants to Plk1 is shown on the left. +++, highest binding affinity to Plk1; -, no binding affinity to Plk1. Myc-Cep85 and its truncated mutants were co-expressed with HA-Plk1 in HEK293T cells followed by co-immunoprecipitation (IP) and immunoblotting (IB) (B) TCL, total cell lysates.

**Figure 5. Continued**

(C) Nek2A binding does not interfere with the interaction of Cep85 and Plk1. Cep85, Plk1-K83M (KM), and different amounts of Nek2A-K37R (KR) were co-expressed in HEK293T cells before co-immunoprecipitation and immunoblotting.

(D) Cep85, Plk1, and Nek2A form a ternary complex in mammalian cells. The procedure of the experiment is outlined in the upper panel, and western blot analysis after two-step immunoprecipitation is shown in the lower panel.

(E) Nek2A depletion does not alter the binding affinity of endogenous Plk1 and Cep85. HEK 293T cells were infected with indicated lentiviral shRNAs before co-immunoprecipitation and immunoblotting with indicated antibodies 48 hr post-infection.

(F) Plk1 inhibition might elevate the binding affinity of endogenous Nek2A and Cep85 in late G2. HeLa cells were synchronized with a double thymidine block. Five hours after releasing, cells were treated with BI2536 for additional 4 hr before co-immunoprecipitation and immunoblotting with indicated antibodies. The binding affinity of Nek2A to Cep85 was quantitated by comparing the amount of Nek2A in the immunoprecipitate (IP) with that in the input, and the results are shown below the representative western blot from three independent experiments.

binding affinity to Plk1, suggesting that aa 34–188 is required for Cep85 to interact with Plk1 (Figures 5A and 5B). However, M6 containing aa 1–256 alone completely lost its binding affinity to Plk1, suggesting that aa 34–188 is not sufficient for Cep85 to bind to Plk1. We thus further extended their length gradually toward the Cep85 C terminus. The binding affinity of these extended truncated mutants including M7-9 were gradually recovered and reached a plateau when it was extended to residue 433 (M10) (Figures 5A and 5B). Therefore the Plk1-binding region is located in Cep85 N-terminal region aa 34–433. In fact, a mutant consisting of aa 34–174 and aa 285–433 largely retained its binding affinity, indicating that Plk1 simultaneously binds to Cep85 in two regions, one around aa 34–187 and the other around aa 257–433.

Given that the NBD (aa 257–433) partially overlaps with Plk1-binding regions (Figure 5A), we were curious to test whether binding of Cep85 to Plk1 and Nek2A were mutually exclusive. To rule out any potential unexpected effects of the kinase activity on their interaction, we chose kinase-dead mutants of Plk1 and Nek2 to perform co-immunoprecipitation assays. Plk1-K82M could specifically interact with Cep85 (Figure 5C). Nek2A-K37R supplemented did not alter the binding affinity of Cep85 and Plk1-K82M even at a high dosage, but rather bound to Cep85 in the same immunoprecipitate (Figure 5C), suggesting that their interaction is not mutually exclusive. In fact, they can form a ternary Plk1-Cep85-Nek2A complex revealed by a two-step immunoprecipitation assay (Figure 5D).

To evaluate the contribution of Nek2A to the interaction between Plk1 and Cep85, we carried out co-immunoprecipitation assays to examine the binding affinity of endogenous Plk1 to Cep85 in the presence or absence of Nek2A. We found that Nek2A depletion did not alter the affinity of endogenous Plk1 and Cep85 (Figure 5E). We further examined whether Plk1 activity would affect the binding affinity of Nek2A and Cep85. When harvesting cells at 9-hr time point after releasing, the binding affinity of endogenous Nek2A and Cep85 might be slightly increased upon BI2536 treatment to inhibit Plk1 activity compared with DMSO treatment in cells (Figure 5F). This result suggests that Plk1 kinase activity may be required for regulating the binding affinity of Cep85 and Nek2A in late G2.

**Nek2A-Assisting Cep85 Phosphorylation by Plk1 Leads to the Dissociation of Phospho-Nek2A from Cep85-Nek2A Complex and Its Activation in Late G2**

Given that Plk1 binding to Cep85 does not simply preclude Nek2A from Cep85-Nek2A complex (Figures 5C and 5D), Plk1 activity might affect the binding affinity between Nek2A and Cep85 (Figures 4H, 4I, and 5F), and both Cep85 and Nek2A can be phosphorylated in late G2 (Mardin et al., 2010) (Figure 3); we thus would like to examine whether phosphorylated Cep85 would alter its binding affinity to phosphorylated Nek2A. We first generated phospho-mimicking mutant Nek2A-4D as well as nonphosphorylatable mutant Nek2A-4A (Figure 6A) according to the previous report (Mardin et al., 2010) and carried out *in vitro* GST pull-down assays to evaluate their binding affinity to the bacterially produced GST-Cep85, which is not supposed to be phosphorylated. Their binding affinity to unphosphorylated GST-Cep85 was indistinguishable (Figure S5A). These Cep85-Nek2A complexes were further subjected to *in vitro* kinase assays. All Nek2A proteins could facilitate Cep85 phosphorylation demonstrated by a distinct mobility shift in the presence of Plk1 and ATP. Among them, Nek2A-4A might be less efficient, revealed by anti-pT392 antibody (Figure 6B). Similar to those shown above (Figure 4H), phosphorylated Cep85 significantly reduced its affinity to Nek2A-WT and Nek2A-K37R with approximately 50% Nek2A proteins remaining on Cep85. In contrast, Nek2A-4A largely retained its affinity to phosphorylated Cep85. Remarkably, only about 20% of Nek2A-4D still remained on phosphorylated Cep85 (Figure 6B). These results indicate that Nek2A-assisting Cep85 phosphorylation by Plk1 will eventually lead to the dissociation of mammalian-cell-expressed Nek2A proteins except for the nonphosphorylatable mutant from the Cep85-Nek2A complex.

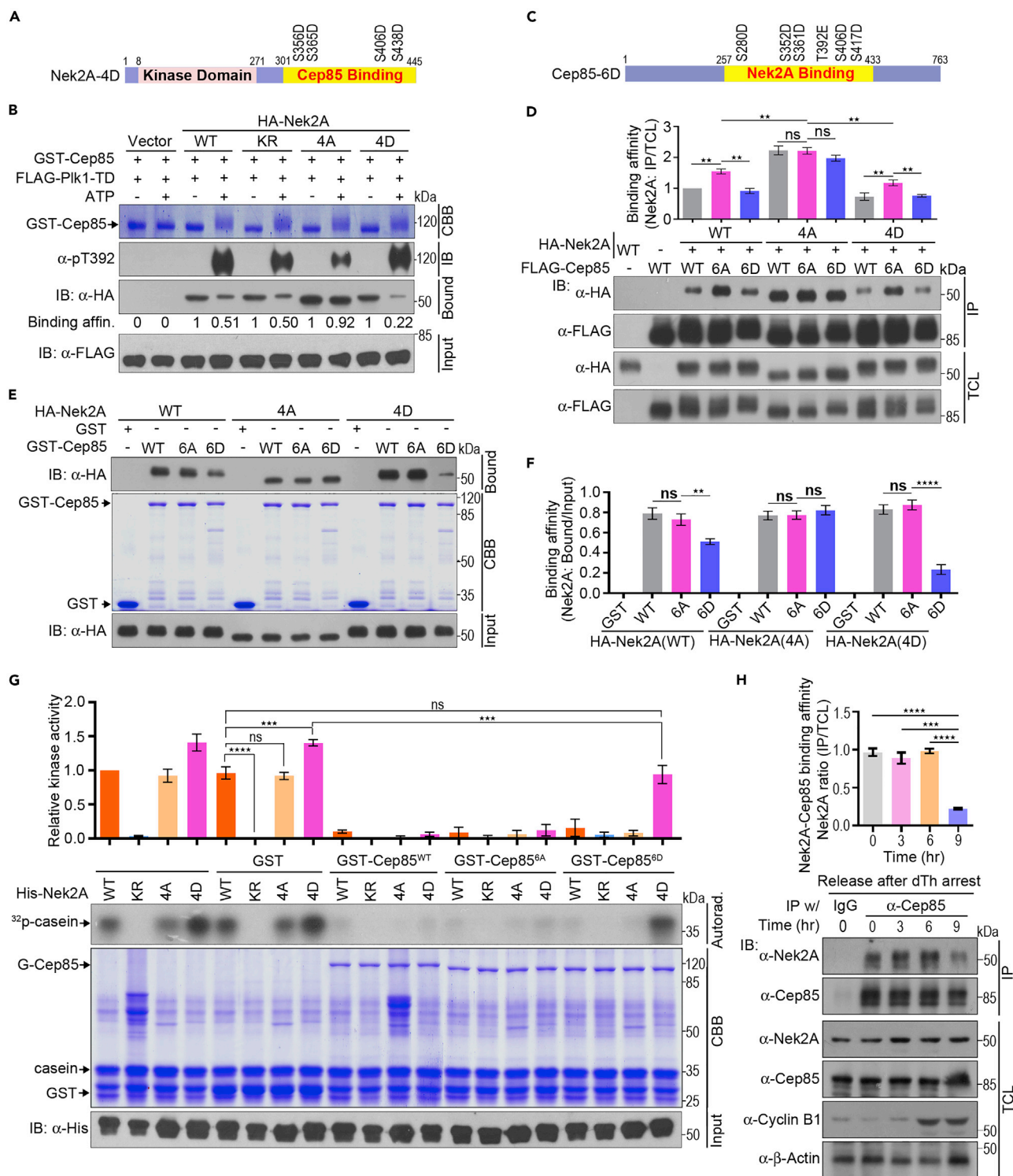


**Figure 6. Nek2A-Assisting Cep85 Phosphorylation by Plk1 Leads to the Dissociation of Phospho-Nek2A from Cep85-Nek2A Complex and Its Activation in Late G2**

(A) Schematic diagram of Nek2A-4D mutant with four phosphorylation sites in Cep85-binding domain mutated to aspartic acid residue. (B) The recombinant GST-Cep85 was incubated with HEK293T cell lysates containing HA-Nek2A proteins before *in vitro* kinase assays. After reaction, the samples were washed to remove unbound proteins before immunoblotting. The relative binding affinity was quantitated by comparing the amount of retained Nek2A in reactions with ATP with that without ATP and is shown below the western blot.

**Figure 6. Continued**

(C) Schematic diagram of Cep85-6D mutant with six phosphorylation sites in the Nek2A-binding domain mutated to the acidic residues.

(D) FLAG-Cep85 and HA-Nek2A constructs were co-transfected into HEK293T cells as indicated. The binding affinity of Nek2A to Cep85, shown in the upper panel, was quantitated by comparing the amount of Nek2A in the immunoprecipitate (IP) with that in the total cell lysates (TCL).

(E and F) (E) GST pull-down assays were performed to evaluate the binding affinity of the recombinant GST-Cep85 proteins to HA-Nek2A proteins overexpressed in HEK293T cells. The binding affinity of Nek2A to GST-Cep85 was quantitated by comparing the amount of Nek2A retained on GST-Cep85 with that in the input and is shown in (F).

(G) The effects of Cep85 mutants on the activity of individual Nek2A kinases were determined by *in vitro* kinase assays with [ $\gamma$ - $^{32}$ P]-ATP. The intensities of autoradiograph bands from three independent experiments were quantified by densitometry and normalized to WT. The relative kinase activity was assessed and is shown in the upper panel.

(H) HeLa cells were synchronized using a double thymidine block. After releasing, cells were harvested at indicated time points before immunoprecipitation of endogenous Cep85 and western blotting (IB) to detect Nek2A in the precipitates (IP) and total cell lysates (TCL). The binding affinity of Nek2A to Cep85 was quantitated by comparing the amount of Nek2A in the immunoprecipitate (IP) with that in TCL and is shown in the upper panel.

For quantitation analysis, data are mean  $\pm$  SEM from three independent experiments. ns, not significant; \*\* $p < 0.01$ , \*\*\* $p < 0.001$ , \*\*\*\* $p < 0.0001$ .

See also [Figure S5](#).

As Plk1 can bulkily phosphorylate Cep85 at multiple sites across the whole protein sequence ([Figure S1](#)), we decided to examine whether the phospho-sites within the NBD were sufficient to regulate its binding affinity to Nek2A. We thus altered all six phosphoserine/threonine residues within this domain to create a phospho-mimicking mutant Cep85-6D and a nonphosphorylatable mutant Cep85-6A ([Figure 6C](#)). *In vitro* kinase assays revealed that Ala replacement could slightly reduce Cep85-6A phosphorylation ([Figure S5B](#)). They were first subjected to co-immunoprecipitation assays to assess their binding affinity to Nek2A proteins ([Figure 6D](#)). Nek2A-4A largely preserved its affinity to Cep85 proteins regardless of their phosphorylation. In contrast, Nek2A-WT and Nek2A-4D significantly reduced their affinity to Cep85 proteins, in particular, Cep85-WT and Cep85-6D. Compared with the Nek2A-4A, Nek2A-WT displayed about 50% reduction of their affinity to Cep85-WT and Cep85-6D, and Nek2A-4D displayed over 60% reduction ([Figure 6D](#)). It is noteworthy that co-expression of Nek2A-WT or Nek2A-4D, but not Nek2A-4A, resulted in a significant mobility shift of all Cep85 proteins ([Figure 6D](#), TCL). Nek2A-WT and Nek2A-4D, but not Nek2A-4A, also displayed a mobility shift. These findings suggest that Cep85-WT and Nek2A-WT are indeed phosphorylated in mammalian cells after they are co-expressed. Therefore the reduction of binding affinity between Cep85-WT and Nek2A-WT is still likely attributed to the electrostatic repulsion between them.

To rule out any unexpected effects on Cep85 when it was co-expressed with Nek2A in mammalian cells, we carried out *in vitro* GST pull-down assays to assess their binding affinity by using recombinant GST-Cep85 proteins, which are not considered to be phosphorylated ([Figures 6E](#) and [6F](#)). We found that Nek2A-4A exhibited nearly equal binding affinity to all GST-Cep85 proteins. GST-Cep85-WT and GST-Cep85-6A fully retained their binding affinity to Nek2A-WT and Nek2A-4D. In contrast, GST-Cep85-6D partially lost its binding affinity to Nek2A-WT and significantly to Nek2A-4D. This discrepancy of their affinity between Nek2A-WT and Nek2A-4D to Cep85-6D may simply be due to the incomplete phosphorylation of Nek2A-WT when it was expressed in mammalian cells.

To address the effect of Cep85 phosphorylation on Nek2A kinase activity, we carried out *in vitro* kinase assays. Similar to our previous report ([Chen et al., 2015](#)), the purified Nek2A-WT from insect cells could specifically phosphorylate  $\beta$ -casein, an artificial Nek2A substrate, and bacterially produced GST-Cep85-WT could efficiently inhibit Nek2A kinase activity ([Figure S5C](#)). As a negative control, the kinase-dead mutant Nek2A-K37R lost its capability to phosphorylate  $\beta$ -casein, whereas Nek2A-4A largely retained its kinase activity ([Figure 6G](#)). In addition, Nek2A-4D displayed a higher kinase activity with about 40% increase compared with Nek2A-WT or Nek2A-4A; however, the exact mechanism is unclear at present. Compared with the GST control, which was shown to have a negligible effect on the activity of Nek2A proteins, supplementation with GST-Cep85 proteins including WT and 6A led to a significant inhibition of the kinase activity of all Nek2A proteins ([Figure 6G](#)). As expected, GST-Cep85-6D protein also efficiently inhibited Nek2A-WT and Nek2A-4A activities. It, however, significantly lost its capability to suppress Nek2A-4D activity. Under this condition, approximately 70% of Nek2A-4D kinase activity was still retained ([Figure 6G](#)), indicating that Cep85 once is phosphorylated will lose its capability to inhibit phospho-Nek2A kinase activity.

Given that both Cep85 and Nek2A are phosphorylated in cells in late G2 ([Mardin et al., 2010](#)) ([Figure 3](#)), we would expect to see that the binding affinity of endogenous Cep85 to Nek2A is significantly decreased at

that stage. We thus synchronized cells and found that the protein levels of Nek2A were steadily increased from G1/S to late G2 (0–9 hr), whereas Cep85 levels remained unchanged at all time points (Figure 6H). The patterns of Cyclin B1 confirmed the efficiency of cell synchronization. Importantly, we found that although Cep85 strongly bound to Nek2A in S phase (3- and 6-hr time point), their binding affinity was significantly decreased with only approximately 20% of Nek2A remaining on Cep85 in late G2 (9-hr time point). Collectively, these *in vitro* and *in vivo* data reveal that phosphorylation of Cep85 by Plk1 will result in the dissociation of phospho-Nek2A from the Cep85-Nek2A complex, thereby tremendously elevating the kinase of phospho-Nek2A in late G2.

### Cep85 Phosphorylation Is Critical for Centrosome Disjunction

Centrosome disjunction is initiated by Nek2A-mediated separation of centrosomes at G2/M and is promoted by the motor protein Eg5-dependent pushing force for the spindle formation in mitosis (Mardin et al., 2010). Therefore to study the contribution of Nek2A to centrosome separation, we have to inhibit Eg5 activity. Eg5 inhibition causes cells to arrest at prometaphase with separated centrosomes (Mardin et al., 2010, 2011). Given that Cep85 phosphorylation diminished its capability to inhibit phospho-Nek2A kinase activity (Figure 6), we decided to examine the contribution of Plk1-mediated Cep85 phosphorylation to the initiation of centrosome disjunction in cells. A series of GFP fusion Cep85 constructs were generated and expressed in a nearly identical level in HeLa cells to evaluate their roles in centrosome disjunction (Figures 7A and 7E). These GFP-Cep85 proteins were able to localize at centrosomes (Figure 7B). When treated with S-trityl-L-cystein (STLC), an inhibitor for Eg5, around 72% of GFP-expressing control cells arrest at prometaphase with a pair of separated centrosomes (Figures 7A–7D). Cep85-WT when overexpressed could significantly suppress centrosome separation, and Cep85-6A further inhibited centrosome separation. In contrast, Cep85-6D lost its capability to prevent centrosome separation (Figures 7A–7D). Therefore to ensure centrosome disjunction, Cep85 has to be phosphorylated by Plk1 at least in its NBD.

To rule out the potential interference of the endogenous Cep85, we employed shRNA technique to deplete the endogenous Cep85 before overexpressing Cep85 proteins and examining their effects on centrosome separation in interphase (Figure 7F). Consistent with the previous report (Chen et al., 2015) and the data shown above (Figure S2), Cep85 depletion resulted in the premature separation of centrosomes with reduced levels of the centrosomal linker protein rootletin (Figure 7G, vector). Expressing siRNA-resistant wild-type Cep85 (SR-WT) or nonphosphorylatable mutant SR-6A largely reversed the effects of Cep85 depletion, displaying the re-connected centrosomes with significantly enhanced rootletin intensity. In contrast, the phospho-mimicking mutant SR-6D partially lost its capability to suppress centrosome splitting under this condition (Figures 7F–7J). We also notice that the capability of SR-6D to prevent centrosome splitting was highly dependent on the timing of analysis. It efficiently suppressed the centrosome splitting at 6 hr, but partially lost its capability at 8 hr and significantly lost at 9 hr after releasing from a double thymidine block (Figures 7F, 7K, and 7L). Given that Nek2A can be phosphorylated by Mst2 and Mst2 has been shown to steadily increase its kinase activity from early G2 (Mardin et al., 2010), we believe that there might exist a reverse correlation between the capability of phospho-Cep85 to suppress centrosome splitting and the levels of phosphorylated Nek2A in interphase cells.

### Both Nek2A and Cep85 Are Required to be Phosphorylated to Ensure Centrosome Separation

To confirm that the capability of phospho-Nek2A to initiate the centrosome disjunction is in fact dependent on the levels of Cep85 phosphorylation, we decided to examine the capability of Cep85 proteins to suppress the centrosome splitting induced by overexpressing phospho-mimicking mutant Nek2A-4D (Figure 8A). We thus first co-expressed GFP as a non-specific control with Nek2A mutants and found that Nek2A-4D, but not Nek2A-4A, could induce centrosome splitting in interphase (Figures 8B–8E). This result is consistent with previous reports (Mardin et al., 2010). When expressed at an identical level, none of Cep85 proteins including Cep85-6D could alter the centrosome cohesion in cells overexpressing Nek2A-4A. However, both Cep85-WT and Cep85-6A could significantly inhibit Nek2A-4D-induced centrosome splitting (Figures 8A–8E). In contrast, Cep85-6D significantly lost its capability to suppress the centrosome splitting induced by Nek2A-4D (Figures 8A–8E). It is noteworthy that Nek2A-4A in all cases resided at centrosomes (Figure 8B), once again suggesting that in addition to its localization at centrosomes, Nek2A phosphorylation is also critical for centrosome disjunction. These results suggest

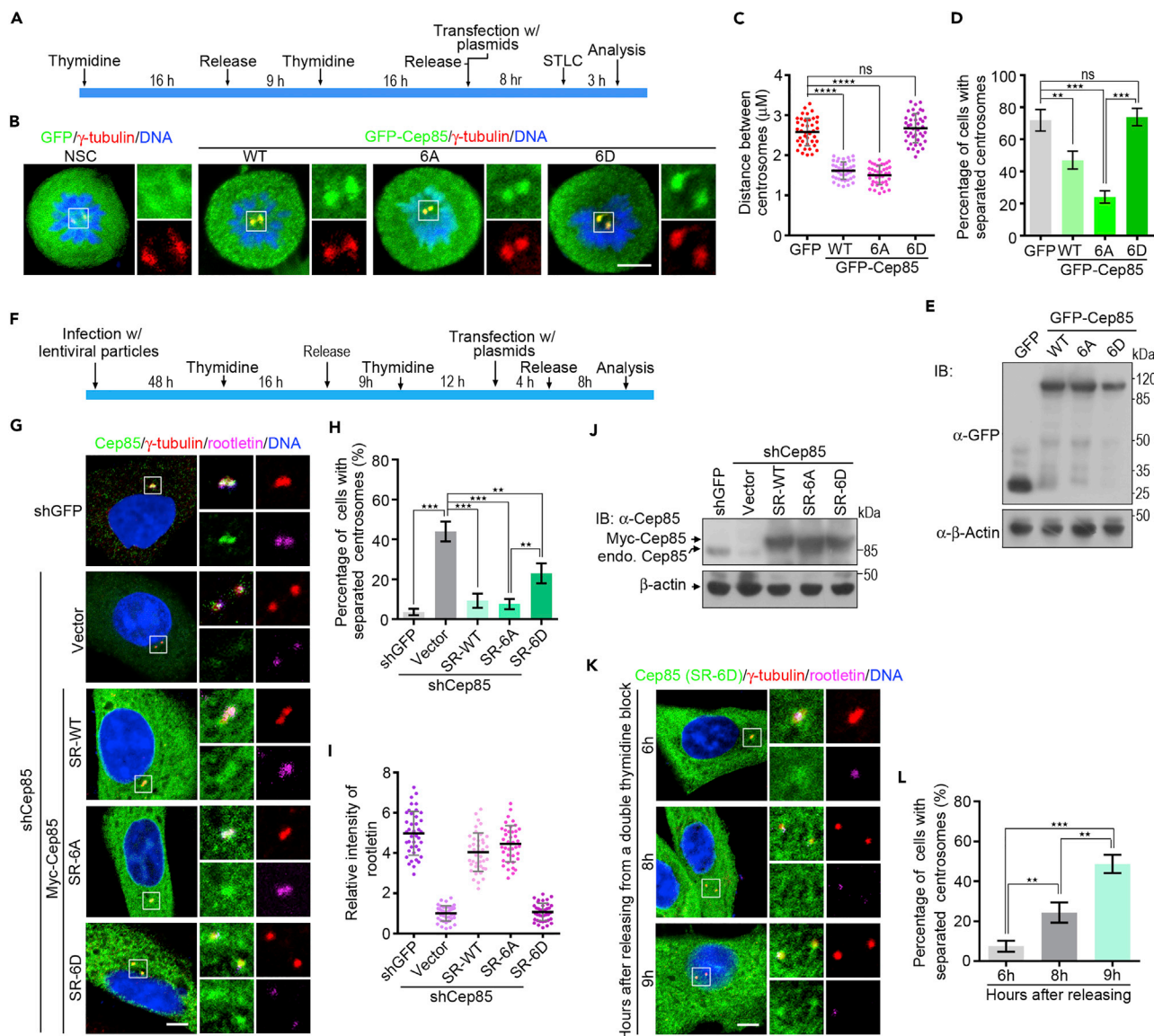


**Figure 7. Cep85 Phosphorylation Is Critical for Centrosome Disjunction**

(A–E) The effects of overexpressed Cep85 proteins on centrosome disjunction. (A) Schematic outline of experiments in (B–E). HeLa cells were enriched at G1/S by a double thymidine block before overexpressing GFP as a control (NSC, non-specific control) or indicated GFP-Cep85 proteins. STLC was used to trap cells in the prometaphase before analysis. (B) The transfected cells were fixed and stained with  $\gamma$ -tubulin (red) to indicate centrosomes. The boxed areas are shown at a higher magnification on the right. The distance between two centrosomes ( $n = 40$ ), percentage of cells with separated centrosomes ( $n = 120$  from three independent experiments), and expression levels of individual proteins in (B) are shown in (C), (D), and (E), respectively.

(F–J) The effects of Cep85 proteins on centrosome splitting resulted from Cep85 depletion. (F) Schematic outline of experiments in (G–J). HeLa cells were infected with indicated lentiviral shRNAs before synchronization with a double thymidine block. Co-transfection with indicated plasmids was performed 4 hr before second release, and analysis was performed 8 hr after releasing. (G) The transfected cells were fixed and stained with antibodies to detect Cep85 (green),  $\gamma$ -tubulin (red), and rootletin (magenta). DNA was stained with DAPI (blue). The boxed areas are shown at a higher magnification on the right. The percentage of cells with separated centrosomes ( $n = 300$  from three independent experiments), relative fluorescent intensity of rootletin ( $n = 40$ ), and expression levels of the endogenous and Myc-tagged Cep85 proteins are shown in (H), (I), and (J), respectively.

(K and L) The experiments were performed exactly according to the schematic outline in (F) with two additional time points (6 and 9 hr). Co-immunostaining and the percentage of cells with separated centrosomes ( $n = 300$  from three independent experiments) are shown in (K) and (L), respectively. For immunostaining, centrosomes are considered separated when the distance between them exceeded  $2 \mu\text{m}$ ; Data are mean  $\pm$  SEM; \*\* $p < 0.01$ ; \*\*\* $p < 0.001$ ; \*\*\*\* $p < 0.0001$ ; scale bar,  $5 \mu\text{m}$ .

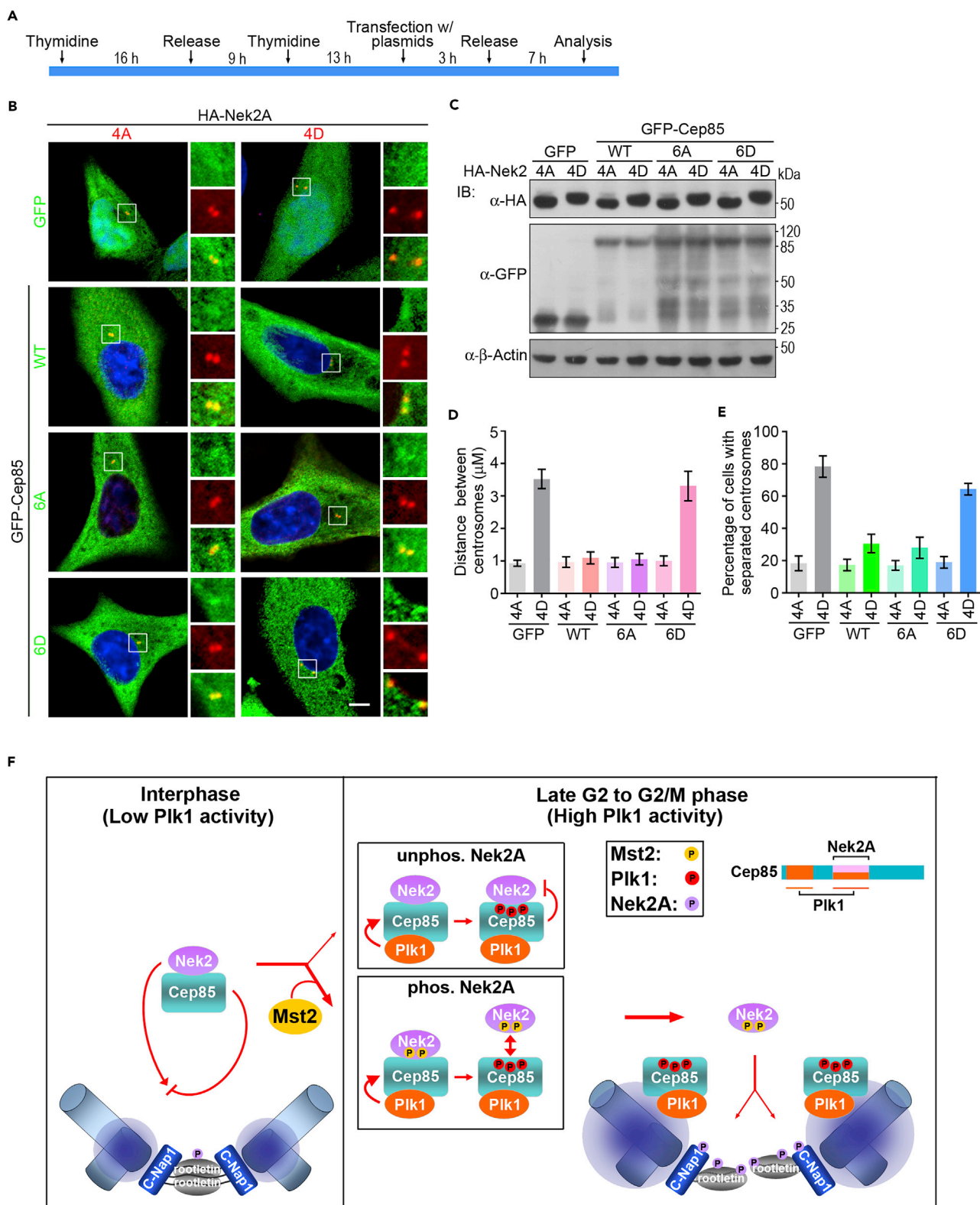


**Figure 8. Continued**

visualize overexpressed HA-Nek2A proteins (red). The boxed areas are shown at a higher magnification on the right. (C) The expression levels of GFP and GFP-Cep85 as well as HA-Nek2A proteins in HeLa cells were examined by western blot. (D) The distance between two centrosomes for cells in (B).  $n = 120$  from three independent experiments. (E) The histogram indicates the percentage of cell with nonseparated centrosomes.  $n = 240$  from three independent experiments. Centrosomes are considered separated when the distance between them exceeded  $2 \mu\text{m}$ . Data are mean  $\pm$  SEM; scale bar,  $5 \mu\text{m}$ . HA, hemagglutinin.

(F) Model for centrosome disjunction regulated by Cep85. At early to mid G2 phase, Cep85 binds to and inhibits Nek2A at centrosomes, thereby preventing Nek2A from phosphorylating intercentrosomal linker consisting of proteins such as C-Nap1 and rootletin. Centrosomes, therefore, remain coherent. As cell cycle progresses into late G2, Cep85 initially still binds to Nek2A regardless of Nek2A phosphorylation, whereas the levels of Nek2A and its phosphorylation mediated by Mst2 kinase at centrosomes are elevated. As Plk1 increases its accumulation at centrosomes and binds to Cep85 to form a ternary complex with Cep85-Nek2A, Cep85 is phosphorylated by Plk1. This leads to the dissociation of phospho-Nek2A exclusively from phosphorylated Cep85 in the complex. Freed phospho-Nek2A initiates centrosome separation by phosphorylating and disassembling the linker between two centrosomes.

that to ensure timely initiation of centrosome separation, both Nek2A and Cep85 have to be phosphorylated in late G2.

**DISCUSSION**

In this study, we have uncovered a previously unrecognized function of Plk1 and Nek2A for Nek2A activation and provided a model to describe this process in centrosome disjunction (Figure 8F). According to our study, it is clear that to achieve a threshold activity at G2/M transition, Nek2A must be phosphorylated. Thereby, once Plk1 binds to Cep85 in Cep85-Nek2A complex, it will phosphorylate Cep85. This in turn leads to the dissociation of phospho-Nek2A from phosphorylated Cep85. Eventually, the freed phospho-Nek2A that is no longer inhibited by Cep85 will initiate centrosome disjunction at G2/M transition. In addition, our study has identified Cep85 as the missing piece to directly relay Plk1 activity to Nek2A for its activation in the mitotic kinase cascades for timely centrosome separation, and has provided further mechanistic insight into the long-standing issue regarding the stringent requirement of phosphorylated Nek2A for centrosome disjunction at G2/M.

It is well known that overactive Nek2A can cause centrosome splitting (Faragher and Fry, 2003; Fry et al., 1998b). As Nek2A protein is steadily increased from S to G2 (Hames et al., 2001; Hayes et al., 2006), its localized activity at centrosomes must be strictly regulated to keep centrosome unseparated in interphase. To date, several proteins have been reported to antagonize Nek2A. These proteins include protein phosphatase 1 PP1 $\alpha$  and pp1 $\gamma$  (Meraldi and Nigg, 2001; Mi et al., 2007), the focal adhesion scaffolding protein HEF1 (Pugacheva and Golemis, 2005), pericentrin (Matsuo et al., 2010), and Cep85 (Chen et al., 2015). However, it is unclear to what extent they contribute to the inhibition of Nek2A activity in interphase and how their antagonism is compromised for centrosome disjunction in late G2 except for PP1 $\gamma$ . Plk1-mediated phosphorylation of Mst2 leads to the dissociation of PP1 $\gamma$  from Mst2-Nek2A-PP1 $\gamma$  complex and activation of Nek2A in late G2 (Mardin et al., 2011). Given that PP1 $\gamma$  was not found to dephosphorylate Nek2A and there are no available data showing that it localizes at centrosomes wherein significant amount of Nek2A resides and functions, we speculate that this might be not the major way for Nek2A to achieve a threshold activity at G2/M transition.

In our previous studies, we have characterized a centrosomal protein Cep85 as a negative regulator to antagonize Nek2A for maintaining the centrosome integrity in interphase (Chen et al., 2015). In this study, we have followed up our study to address their interaction in late G2. In the mechanistic study, we were initially surprised to see that Plk1 cannot phosphorylate the recombinant Cep85 protein (Figure 4F). It becomes reasonable when we realized the facts that Nek2A indeed is complexed with Cep85 at centrosomes in cells and Nek2A binding is pre-required for Cep85 to be phosphorylated by Plk1 (Figure 4) (Chen et al., 2015). The facts that both Cep85 and Nek2A are phosphorylated in late G2 and Nek2A is actively involved in Cep85 phosphorylation for its own activation highly suggest that Cep85 is a primary antagonist for Nek2A in interphase that has to be overcome in late G2 (Figures 3, 4, 5, 6, 7, and 8) (Mardin et al., 2010). Recently, Cep85 has also been found to bind to STIL to regulate Plk4 activation during centriole duplication (Liu et al., 2018). The interaction of Cep85 and STIL seems to be transient and occurs in the early phase of centriole duplication. It would be interesting to examine whether this portion of Cep85 plays a role by transferring from STIL to Nek2A to prevent premature centrosome separation once it accomplishes its mission during centriole duplication. This hypothesis

could be examined by determining Cep85 localization at centrosomes with high resolution after the G1/S transition.

In interphase, the centrosomes are held together by a proteinaceous linker consisting of a number of proteins, such as C-Nap1 and rootletin, and are disjoined by Nek2A-mediated phosphorylation of these linker proteins in late G2 (Bahe et al., 2005; Hardy et al., 2014; Mardin and Schiebel, 2012). Recent studies have revealed a highly regulated kinase cascade CDK1-AurA-Plk1-Nek2A to ensure the timely centrosome separation (Cosenza and Kramer, 2016; Wang et al., 2014). In this cascade, Plk1 is not reported to activate Nek2A directly but to increase Nek2A activity indirectly by phosphorylating the kinase Mst2, a component of the hippo pathway (Mardin et al., 2011). Plk1-dependent phosphorylation of Mst2 results in the dissociation of PP1 $\gamma$  from the Mst2-Nek2A-PP1 $\gamma$  complex, thereby preventing PP1 $\gamma$  from dephosphorylating c-Nap1 and indirectly increasing Nek2A activity. It is well known that phosphorylation of Thr180 within the activation loop of Mst2 is crucial for its activation (Deng et al., 2003; Galan and Avruch, 2016). Given that Plk1-mediated phosphorylation of Mst2 occurs at three additional sites other than this critical residue, it remains obscure whether Plk1-induced Mst2 phosphorylation also leads to an increase in Mst2 kinase activity that is responsible for Nek2A phosphorylation in late G2 (Mardin et al., 2010, 2011). Overall, these studies seem to favor the idea that Plk1 can activate Nek2A in an indirect manner.

In our current study, we have provided several lines of evidence to support the argument that Plk1 can indeed directly activate Nek2A through Cep85 in late G2. We have shown that Plk1 can bind to Cep85 and form a ternary Plk1-Cep85-Nek2A complex (Figures 1 and 5). Both Plk1 and Nek2A are required for Cep85 phosphorylation *in vitro* and *in vivo* (Figures 2, 3, and 4). Nek2A is actively involved in Plk1-mediated Cep85 phosphorylation by converting Cep85 to an excellent substrate for Plk1 by forming a Cep85-Nek2A complex (Figure 4). In addition, Nek2A-assisting Cep85 phosphorylation leads to the dissociation of phospho-Nek2A from Cep85-Nek2A antagonizing complex and the activation of freed phospho-Nek2A (Figure 6). It thus becomes clear that to overcome Cep85 antagonism at G2/M transition, Nek2A must first increase its accumulation at centrosomes and then has to be phosphorylated, which is mediated by Mst2 (Mardin et al., 2010), although it remains unknown how exactly Mst2 is activated in late G2 (Hergovich and Hemmings, 2012). It also becomes clear that Plk1 at centrosomes plays pivotal regulatory roles in the initiation of centrosome disjunction by activating phospho-Nek2A directly by phosphorylating Cep85 and indirectly by inhibiting PP1 $\gamma$ .

In summary, our results identify Cep85 as a platform to directly relay the activities of Plk1 and Mst2 to Nek2A activation at centrosomes through phospho-Nek2A-assisted Cep85 phosphorylation by Plk1 at the onset of mitosis.

### Limitations of the Study

In this study we have clearly demonstrated that both Plk1 and Nek2A are necessary for Cep85 phosphorylation *in vitro* and *in vivo*. However, we have not yet examined whether they are sufficient for Cep85 phosphorylation because of the lack of the bacterially expressed recombinant Plk1 and Nek2A proteins. We thus do not know whether other centrosome-residing proteins, such as Mst2, are also involved in this process. It would be helpful to further clarify the events that occurred at the G2/M transition during centrosome disjunction if we could solve the problem in our future study.

### METHODS

All methods can be found in the accompanying [Transparent Methods supplemental file](#).

### DATA AND SOFTWARE AVAILABILITY

Our dataset of the raw data of Western blotting in Mendeley Data at <https://doi.org/10.17632/9b6jg26ym2.1>

### SUPPLEMENTAL INFORMATION

Supplemental Information includes Transparent Methods and five figures and can be found with this article online at <https://doi.org/10.1016/j.isci.2018.12.013>.

## ACKNOWLEDGMENTS

This work was supported by the National Natural Science Foundation of China (grant numbers 31771488 to C.C. and 31471260 to X.Y.). We thank Dr. Dawang Zhou for critical comments on the manuscript.

## AUTHOR CONTRIBUTIONS

Conceptualization, C.C. and X.Y.; Methodology, C.C.; Investigation, C.C., Z.X., T.Z., L.L., M.L., and C.X.; Writing – Original Draft, C.C. and X.Y.; Writing – Review & Editing, C.C. and X.Y.; Funding Acquisition, C.C. and X.Y.; Resources, C.C. and X.Y.; Supervision, C.C. and X.Y.

## DECLARATION OF INTERESTS

The authors declare no competing interests.

Received: August 21, 2018

Revised: November 19, 2018

Accepted: December 17, 2018

Published: January 25, 2019

## REFERENCES

- Avidor-Reiss, T., and Gopalakrishnan, J. (2013). Building a centriole. *Curr. Opin. Cell Biol.* 25, 72–77.
- Azimzadeh, J., and Bornens, M. (2007). Structure and duplication of the centrosome. *J. Cell Sci.* 120, 2139–2142.
- Bahe, S., Stierhof, Y.D., Wilkinson, C.J., Leiss, F., and Nigg, E.A. (2005). Rootletin forms centriole-associated filaments and functions in centrosome cohesion. *J. Cell Biol.* 171, 27–33.
- Bettencourt-Dias, M., and Glover, D.M. (2007). Centrosome biogenesis and function: centrosomics brings new understanding. *Nat. Rev. Mol. Cell Biol.* 8, 451–463.
- Bornens, M. (2012). The centrosome in cells and organisms. *Science* 335, 422–426.
- Bruinsma, W., Raaijmakers, J.A., and Medema, R.H. (2012). Switching Polo-like kinase-1 on and off in time and space. *Trends Biochem. Sci.* 37, 534–542.
- Chen, C., Tian, F., Lu, L., Wang, Y., Xiao, Z., Yu, C., and Yu, X. (2015). Characterization of Cep85—a new antagonist of Nek2A that is involved in the regulation of centrosome disjunction. *J. Cell Sci.* 128, 3290–3303.
- Cosenza, M.R., and Kramer, A. (2016). Centrosome amplification, chromosomal instability and cancer: mechanistic, clinical and therapeutic issues. *Chromosome Res.* 24, 105–126.
- Deng, Y., Pang, A., and Wang, J.H. (2003). Regulation of mammalian STE20-like kinase 2 (MST2) by protein phosphorylation/dephosphorylation and proteolysis. *J. Biol. Chem.* 278, 11760–11767.
- Faragher, A.J., and Fry, A.M. (2003). Nek2A kinase stimulates centrosome disjunction and is required for formation of bipolar mitotic spindles. *Mol. Biol. Cell* 14, 2876–2889.
- Fry, A.M., Mayor, T., Meraldi, P., Stierhof, Y.D., Tanaka, K., and Nigg, E.A. (1998a). C-Nap1, a novel centrosomal coiled-coil protein and candidate substrate of the cell cycle-regulated protein kinase Nek2. *J. Cell Biol.* 141, 1563–1574.
- Fry, A.M., Meraldi, P., and Nigg, E.A. (1998b). A centrosomal function for the human Nek2 protein kinase, a member of the NIMA family of cell cycle regulators. *EMBO J.* 17, 470–481.
- Galan, J.A., and Avruch, J. (2016). MST1/MST2 protein kinases: regulation and physiologic roles. *Biochemistry* 55, 5507–5519.
- Graser, S., Stierhof, Y.D., and Nigg, E.A. (2007). Cep68 and Cep215 (Cdk5rap2) are required for centrosome cohesion. *J. Cell Sci.* 120, 4321–4331.
- Hames, R.S., Wattam, S.L., Yamano, H., Bacchieri, R., and Fry, A.M. (2001). APC/C-mediated destruction of the centrosomal kinase Nek2A occurs in early mitosis and depends upon a cyclin A-type D-box. *EMBO J.* 20, 7117–7127.
- Hardy, T., Lee, M., Hames, R.S., Prosser, S.L., Cheary, D.M., Samant, M.D., Schultz, F., Baxter, J.E., Rhee, K., and Fry, A.M. (2014). Multisite phosphorylation of C-Nap1 releases it from Cep135 to trigger centrosome disjunction. *J. Cell Sci.* 127, 2493–2506.
- Hayes, M.J., Kimata, Y., Wattam, S.L., Lindon, C., Mao, G., Yamano, H., and Fry, A.M. (2006). Early mitotic degradation of Nek2A depends on Cdc20-independent interaction with the APC/C. *Nat. Cell Biol.* 8, 607–614.
- He, R., Huang, N., Bao, Y., Zhou, H., Teng, J., and Chen, J. (2013). LRRC45 is a centrosome linker component required for centrosome cohesion. *Cell Rep.* 4, 1100–1107.
- Hergovich, A., and Hemmings, B.A. (2012). Hippo signalling in the G2/M cell cycle phase: lessons learned from the yeast MEN and SIN pathways. *Semin. Cell Dev. Biol.* 23, 794–802.
- Liu, X., and Erikson, R.L. (2002). Activation of Cdc2/cyclin B and inhibition of centrosome amplification in cells depleted of Plk1 by siRNA. *Proc. Natl. Acad. Sci. U S A* 99, 8672–8676.
- Liu, Y., Gupta, G.D., Barnabas, D.D., Agircan, F.G., Mehmood, S., Wu, D., Coyaud, E., Johnson, C.M., McLaughlin, S.H., Andreeva, A., et al. (2018). Direct binding of CEP85 to STIL ensures robust PLK4 activation and efficient centriole assembly. *Nat. Commun.* 9, 1731.
- Macurek, L., Lindqvist, A., Lim, D., Lampson, M.A., Klompaker, R., Freire, R., Clouin, C., Taylor, S.S., Yaffe, M.B., and Medema, R.H. (2008). Polo-like kinase-1 is activated by aurora A to promote checkpoint recovery. *Nature* 455, 119–123.
- Mardin, B.R., Agircan, F.G., Lange, C., and Schiebel, E. (2011). Plk1 controls the Nek2A-PP1gamma antagonism in centrosome disjunction. *Curr. Biol.* 21, 1145–1151.
- Mardin, B.R., Lange, C., Baxter, J.E., Hardy, T., Scholz, S.R., Fry, A.M., and Schiebel, E. (2010). Components of the Hippo pathway cooperate with Nek2 kinase to regulate centrosome disjunction. *Nat. Cell Biol.* 12, 1166–1176.
- Mardin, B.R., and Schiebel, E. (2012). Breaking the ties that bind: new advances in centrosome biology. *J. Cell Biol.* 197, 11–18.
- Matsuo, K., Nishimura, T., Hayakawa, A., Ono, Y., and Takahashi, M. (2010). Involvement of a centrosomal protein kendrin in the maintenance of centrosome cohesion by modulating Nek2A kinase activity. *Biochem. Biophys. Res. Commun.* 398, 217–223.
- Meraldi, P., and Nigg, E.A. (2001). Centrosome cohesion is regulated by a balance of kinase and phosphatase activities. *J. Cell Sci.* 114 (Pt 20), 3749–3757.
- Mi, J., Guo, C., Brautigan, D.L., and Larner, J.M. (2007). Protein phosphatase-1alpha regulates centrosome splitting through Nek2. *Cancer Res.* 67, 1082–1089.

Nigg, E.A., and Raff, J.W. (2009). Centrioles, centrosomes, and cilia in health and disease. *Cell* 139, 663–678.

Parrilla, A., Cirillo, L., Thomas, Y., Gotta, M., Pintard, L., and Santamaria, A. (2016). Mitotic entry: the interplay between Cdk1, Plk1 and Bora. *Cell Cycle* 15, 3177–3182.

Pugacheva, E.N., and Golemis, E.A. (2005). The focal adhesion scaffolding protein HEF1 regulates activation of the Aurora-A and Nek2 kinases at the centrosome. *Nat. Cell Biol.* 7, 937–946.

Seki, A., Coppinger, J.A., Jang, C.Y., Yates, J.R., and Fang, G. (2008). Bora and the kinase Aurora a cooperatively activate the kinase Plk1 and control mitotic entry. *Science* 320, 1655–1658.

Smith, E., Hegarat, N., Vesely, C., Roseboom, I., Larch, C., Streicher, H., Straatman, K., Flynn, H., Skehel, M., Hirota, T., et al. (2011). Differential control of Eg5-dependent centrosome separation by Plk1 and Cdk1. *EMBO J.* 30, 2233–2245.

van Ree, J.H., Nam, H.J., and van Deursen, J.M. (2016). Mitotic kinase cascades orchestrating timely disjunction and movement of centrosomes

maintain chromosomal stability and prevent cancer. *Chromosome Res.* 24, 67–76.

Wang, G., Jiang, Q., and Zhang, C. (2014). The role of mitotic kinases in coupling the centrosome cycle with the assembly of the mitotic spindle. *J. Cell Sci.* 127, 4111–4122.

Yang, J., Adamian, M., and Li, T. (2006). Rootletin interacts with C-Nap1 and may function as a physical linker between the pair of centrioles/basal bodies in cells. *Mol. Biol. Cell* 17, 1033–1040.

**ISCI, Volume 11**

**Supplemental Information**

**Cep85 Relays Plk1 Activity  
to Phosphorylated Nek2A for Its Timely  
Activation in Centrosome Disjunction**

**Canhe Chen, Zhenping Xu, Ting Zhang, Liping Lin, Mingke Lu, Changchuan Xie, and Xianwen Yu**

## Supplemental Information

### Supplemental Figures

**Figure S1**

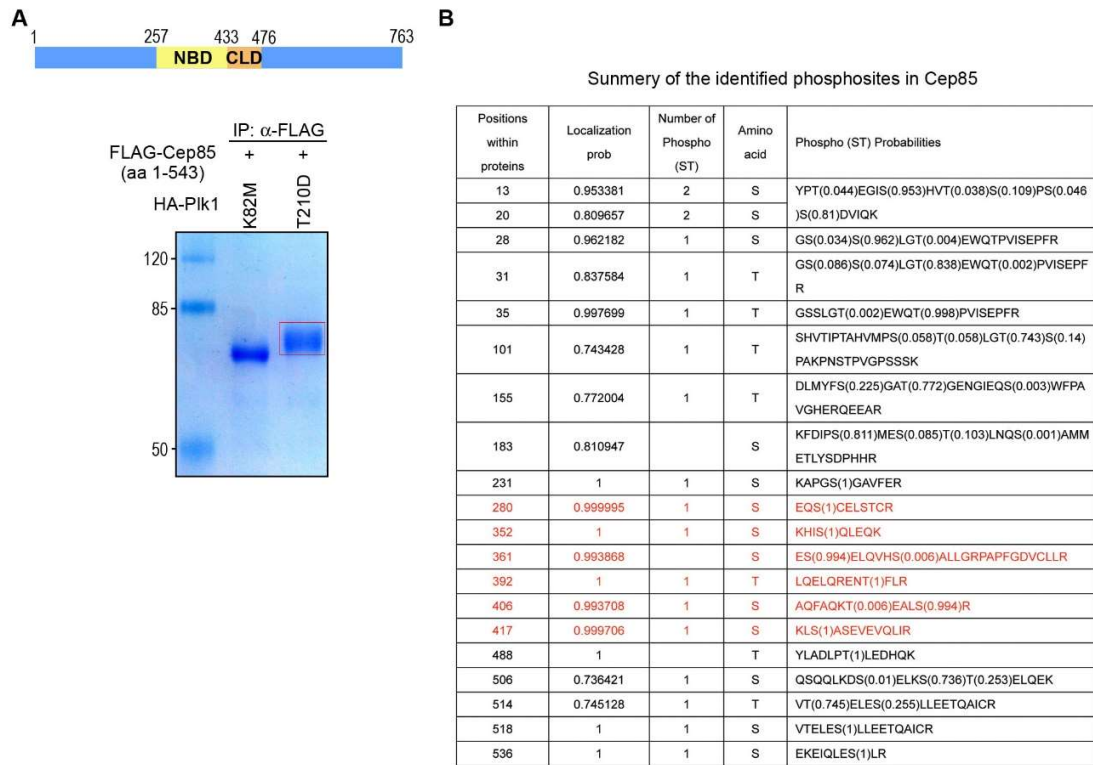


**Figure S1. Identification of the phospho-sites in Cep85. Related to Figure 3.**

(A) A schematic diagram of Cep85 and its domains is shown in the upper panel. NBD, the Nek2A binding domain; CLD, the centrosome localization domain. A truncated mutant of Cep85 (aa 1-543), co-expressed with active Plk1-T210D or inactive Plk1-K82M, was immunoprecipitated from HEK293T cell lysates and separated on an SDS-PAGE, followed by Coomassie brilliant blue (CBB) staining to visualize the Cep85 protein. The protein bands inside the red boxed area were excised and sent for identification of phospho-sites by mass spectrometry.

(B) Summary of phospho-sites in Cep85 identified by mass spectrometry. Highlighted in red are the residues that were mutated for its functional study in the following-up experiments.

**Figure S2**

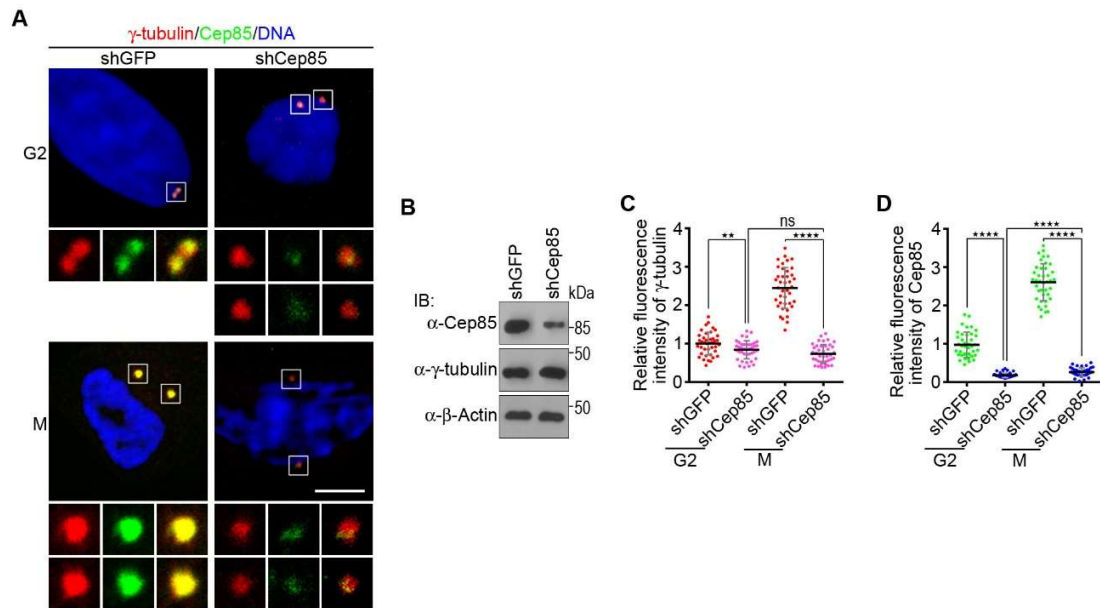


**Figure S2. The effects of Cep85 depletion. Related to Figure 4.**

(A) Immunostaining confirms the efficiency of shCep85-mediated Cep85 depletion. HeLa cells were infected with either shGFP (control) or shCep85 lentiviral particles 72 h prior to immunostaining with anti-Cep85 (green) and anti- $\gamma$ -tubulin (red). The boxed areas are shown at a higher magnification directly below the corresponding image.

(B) Depletion of Cep85 does not alter  $\gamma$ -tubulin levels in HeLa cells. Cells were infected with either shGFP (control) or shCep85 lentiviral particles 72 h prior to Western blot analysis.

The relative fluorescent intensities of  $\gamma$ -tubulin and Cep85 in (A) were quantitated and plotted in (C) and (D), respectively.  $n=40$  for each group. Data are mean  $\pm$  s.e.m.; ns, not significant; \*\* $p<0.01$ ; \*\*\*\* $p<0.0001$ . Scale bar represents 5  $\mu$ m.

**Figure S3**

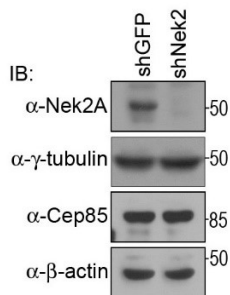


**Figure S3. Nek2A depletion does not alter the total levels of  $\gamma$ -tubulin and Cep85 in cells. Related to Figure 4.**

HeLa cells were infected with the indicated lentiviral shRNAs for 36 h prior to immunoblotting with indicated antibodies.

**Figure S4**

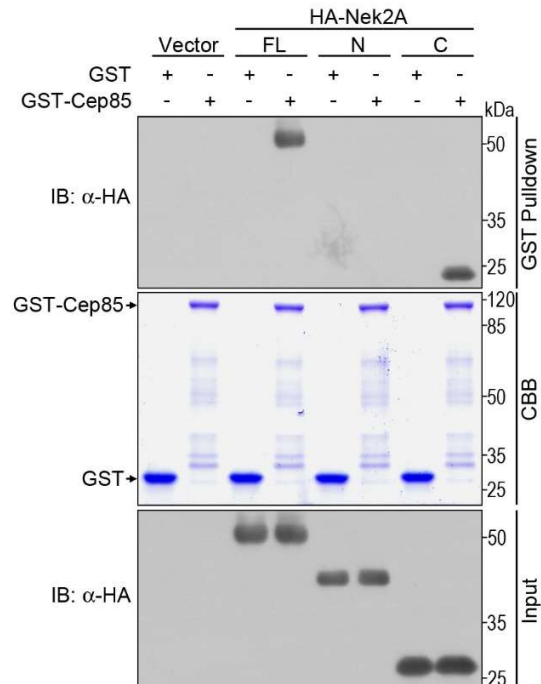


**Figure S4. Recombinant GST-Cep85 protein binds to the full-length as well as C-terminal region of Nek2A. Related to Figure 4.**

Bacterially produced GST-Cep85 protein was incubated with HEK293T cell lysates containing HA-Nek2A proteins including full-length (FL), N-terminal region containing the kinase domain (aa 1-300, N) and C-terminal region containing Mst2-mediated phospho-sites (aa 301-445, C). GST pull-down assays and Western blot analysis were subsequently performed to reveal their binding affinity. CBB, Coomassie brilliant blue stain.

**Figure S5**

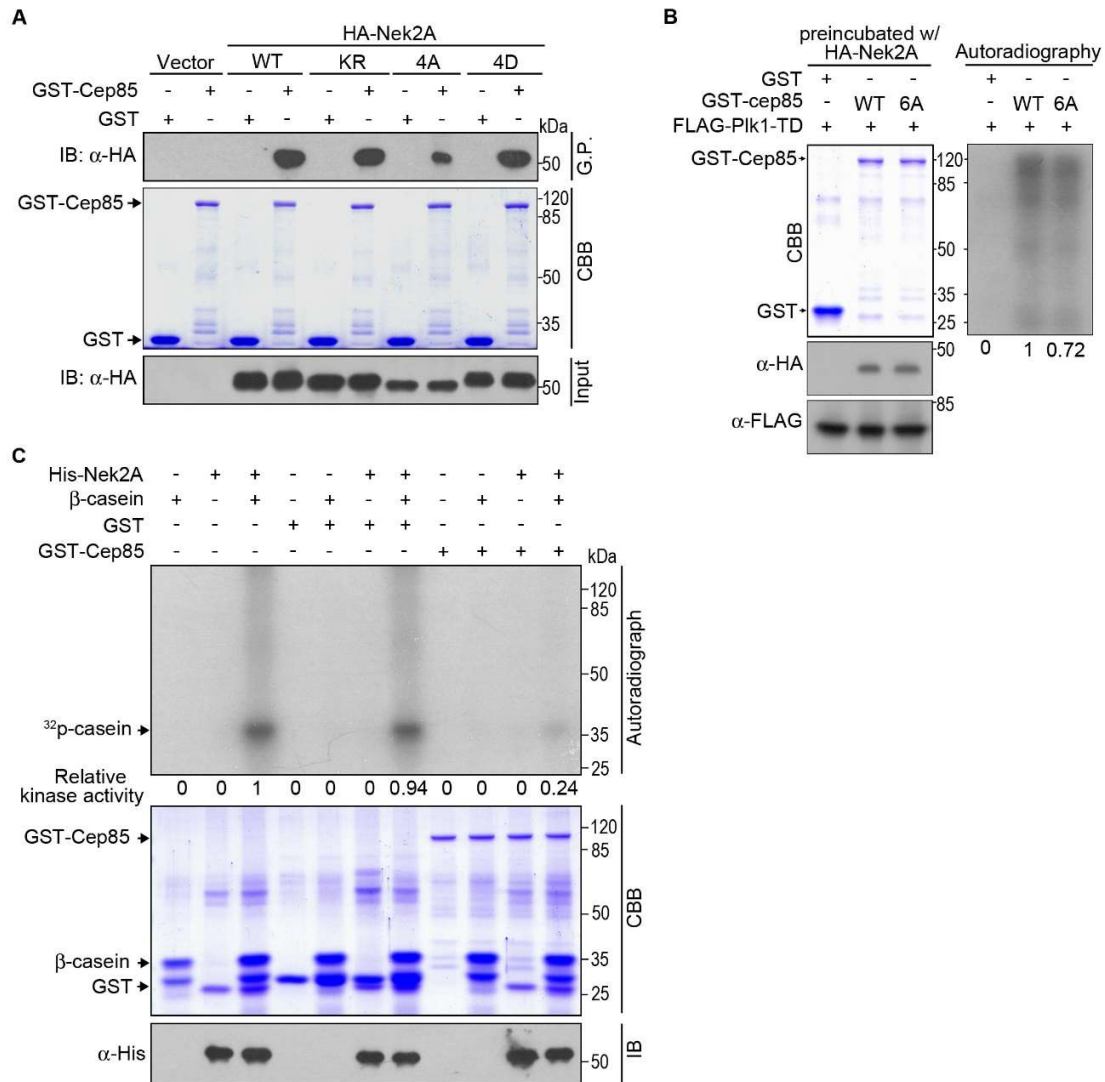


**Figure S5. Interaction between Cep85 and Nek2A. Related to Figure 6.**

(A) Nek2A mutants bind to Cep85 with an affinity similar to Nek2A-WT. In vitro GST pull-down assays and Western blotting were carried out to evaluate the binding affinity between recombinant GST-Cep85 and Nek2A proteins overexpressed in HEK293T cells.

(B) Plk1 displays a less efficiency to phosphorylate the nonphosphorylatable mutant Cep85-6A. Recombinant GST-Cep85-WT and GST-Cep85-6A proteins were incubated with HEK239T cell lysate containing overexpressed HA-Nek2A prior to in vitro kinase assays with  $[\gamma\text{-}^{32}\text{P}]\text{-ATP}$ . Autoradiography was used to evaluate the incorporation of  $[\text{}^{32}\text{P}]$  into GST-Cep85, and Western blotting was used to reveal the bound HA-Nek2A proteins and FLAG-Plk1 used in the kinase reaction.

(C) Cep85 can inhibit Nek2A kinase activity. The kinase activity of the purified recombinant His-Nek2A was determined using in vitro kinase assays with  $\beta$ -casein as a substrate. The autoradiography

shows [<sup>32</sup>P]-β-casein. Purified recombinant GST–Cep85, GST and β-casein were visualized by Coomassie brilliant blue (CBB) stain.

## TRANSPARENT METHODS

### Plasmid constructions

The mammalian expression plasmids for Cep85 and Nek2A, peGFP-C2-Cep85 (WT) and pFastBac-HTA-Nek2A (WT) were as described(Chen et al., 2015). Human Plk1 coding sequence was amplified from a cDNA library prepared by reverse transcription of total RNA isolated from HEK293T cells and subcloned into the mammalian expression vector pCMV5-HA. This construct was verified by full-length sequencing and further subcloned into mammalian expression vectors pcDNA3.3-Myc and -FLAG. Cep85, Plk1 and Nek2A point mutations were created by PCR-based site-directed mutagenesis using plasmids based on the pcDNA3.3-HA vector as templates as described previously(Chen et al., 2015). These inserts were further subcloned into pcDNA3.3-Myc and -FLAG vectors. The truncated mutants of Cep85 were generated by PCR amplification and subcloned into pcDNA3.3-Myc vector. GST fusion and GFP fusion plasmids were created by releasing the individual inserts from pcDNA3.3-HA vector using restriction enzymes and subcloned into pGEX-4T-1 and peGFP-C2 vectors. Plk1 and Nek2A mutants were also subcloned into the donor vector pFastBac-HTA (Invitrogen) for expressing recombinant His-tagged proteins in insect cells. The siRNA-resistant Cep85 wildtype and mutant constructs were created by the PCR-based mutagenesis with primers containing silence mutations against siCep85-targeting sequence, 5'-CCA TGT GAT GCC TTC TAC TTT-3'. The sequence harboring multiple silence mutations against siCep85-recognizing sequence in these siRNA-resistant Cep85 constructs is 5'-ACA CGT TAT GCC AAG CAC ATT-3'. Primer sequences used for PCR amplification and mutagenesis are available on request. All constructs were confirmed by sequencing.

### Cell lines and treatments

Human cervical cancer HeLa and HEK293T cell lines were purchased from the ATCC. Cells were grown in a high-glucose Dulbecco's modified Eagle's medium (Hyclone) plus 10% fetal bovine serum (Gemini) and 100 IU/ml penicillin and 100 µg/ml streptomycin at 37°C in a humidified 5% CO<sub>2</sub> incubator. Transient transfection of HEK293T was carried out with the cationic polymer polyethylenimine (PEI) as described previously(Chen et al., 2015). TurboFect reagent (Thermo Scientific) was used to transfect HeLa cells according to the manufacturer's instruction.

The double thymidine block was carried out as follows: cells were first incubated for 16 h with 2.5 mM thymidine followed by three quick washes with PBS and release in thymidine-free medium for 9 h. They were further incubated with 2.5 mM thymidine for an additional 16 h. Cells were washed three times with PBS, returned to fresh medium and allowed to grow for 0–16 h before harvesting the synchronized cells at different stages of cell cycle for analysis. To arrest cells at prometaphase, 10 µM S-trityl-L-cysteine (STLC) was added to the medium 8 h after transfection. To Inhibit Plk1 activity, 50 nM of BI2536 was used for HeLa cells.

### **shRNA sequences and lentivirus expression system**

Primers for Cep85 shRNA (sh-1, 5'-CCG GCC ATG TGA TGC CTT CTA CTT TCT CGA GAA AGT AGA AGG CAT CAC ATG GTT TTT TG-3'; sh-2, 5'-AAT TCA AAA AAC CAT GTG ATG CCT TCT ACT TTC TCG AGA AAG TAG AAG GCA TCA CAT GG-3'), for Nek2A shRNA (sh-1, 5'-CCG GGC CAT GCC TTT CTG TAT AGT ACT CGA GTA CTA TAC AGA AAG GCA TGG CTT TTT TG-3'; sh-2, 5'-AAT TCA AAA AAG CCA TGC CTT TCT GTA TAG TAC TCG AGT ACT ATA CAG AAA GGC ATG GC-3'), and for Plk1 shRNA (sh-1, 5'-CCG GAA CGA GCT GCT TAA TGA CGA GCT CGA GCT CGT CAT TAA GCA GCT CGT TTT TTT G-3'; sh-2, 5'-AAT TCA AAA AAA CGA GCT GCT TAA TGA CGA GCT CGA GCT CGT CAT TAA GCA GCT CGT T-3') were purchased from Boray Biotechnology (Xiamen, China). Primer pair were annealed and the shRNA double-stranded oligonucleotides were cloned into lentiviral pLKO.1-TRC vector digested with AgeI and EcoRI. The plasmid pLKO.1 GFP shRNA, a gift from David Sabatini (Sancak et al., 2008), was used as a non-specific control. Recombinant lentivirus was produced by transient transfection of HEK293T cells using the 3<sup>rd</sup> generation lentiviral system following a standard protocol.

### **Immunofluorescence microscopy**

For immunofluorescence, except those cells expressing GFP or GFP fusion protein that were fixed with 0.15% PFA for 1h at room temperature prior to the methanol fixation, HeLa cells were fixed with ice-cold methanol for 7 min, blocked with 5% (v/v) bovine serum albumin (BSA) and 0.075% Triton X-100 in PBS for at least 30 min. Cells were subsequently incubated with primary antibodies with 5% (v/v) BSA and 0.075% Triton X-100 in PBS for 1.5 h followed by three washes with 0.075% Triton X-100 in PBS for a total of 30 min and another 1.5 h incubation with secondary antibodies diluted in PBS with 5% (v/v) BSA and 0.075% Triton X-100. DNA was stained with DAPI (0.2 µg/ml; Invitrogen). Primary antibodies included rabbit anti-Cep85 (26314-1-AP, Proteintech; 1:100), mouse anti-Nek2 (BD Biosciences; 1:200), mouse anti-Plk1 (ab 17057, Abcam; 1:1,000), mouse anti-Cep85 (SAB1407896, Sigma; 1:1,000), rabbit anti-pericentrin (ab4448, Abcam; 1:2,500), rabbit anti-Cep85pT392 (Raised by Genescript; 1:2,500), mouse anti-γ-tubulin (T6557, Sigma-Aldrich; 1:2,000), and rabbit anti-HA-tag (H6908, Sigma-Aldrich; 1:500). Secondary antibodies included donkey anti-mouse-IgG conjugated to Alexa Fluor 488 (Invitrogen; 1:1,000), donkey anti-rabbit-IgG conjugated to Alexa Fluor 488 (Invitrogen; 1:1,000), donkey anti-mouse-IgG conjugated to Alexa Fluor 555 (Invitrogen; 1:2,000) and donkey anti-rabbit-IgG conjugated to Alexa Fluor 555 (Invitrogen; 1:2,000). Images were acquired using a Zeiss LSM 780 laser-scanning confocal microscope (Carl Zeiss, Germany), equipped with a 100×/1.40 Plan-Apochromat objective.

Based on the intensity of centrosomal marker staining and the distance of centrosomes as well as nuclear morphology, cells were categorized into their respective stages. Those cells with unseparated centrosomes in G2 were further classified to be at G2/M if the fluorescent intensity of Cep85 is over 2.5 folds higher than that in G1.

### **Immunoprecipitation and Western blotting**

For immunoprecipitation, briefly, mammalian cells were lysed in the ice-cold cell lysis buffer

containing 50 mM Tris-HCl pH 7.4, 150 mM NaCl, 1 mM EDTA and 0.5% NP-40, supplemented with 10 µg/ml pepstatin A, 10 µg/ml leupeptin and 1 mM PMSF. Cleaned cell lysates were incubated with antibodies at 4°C for 2 h prior to incubation with Protein A/G PLUS-Agarose (Santa Cruz Biotechnology) for an extra 2 h. To pull down FLAG-tagged protein from cell lysates, anti-FLAG M2 affinity gel (Sigma) was used with 4-h incubation. For the endogenous protein immunoprecipitation, overnight incubation was employed. The immunoprecipitates were washed, boiled in 1x SDS sample buffer containing 62.5 mM Tris-HCl (pH 6.8), 2% SDS, 10% glycerol, 50 mM DTT and 0.01% bromophenol blue, resolved by an SDS-PAGE and transferred onto a PVDF membrane (Millipore) prior to Western blot analysis. Antibodies used for one immunoprecipitation incubation included: rabbit anti-Cep85 (26314-1-AP, Proteintech; 1µg), anti-FLAG M2 affinity gel (F2426, Sigma: 3 µl); mouse anti-HA (SC-7329, Santa Cruz Biotechnology; 1 µg).

To detect phosphorylation of endogenous Cep85, samples were prepared by directly harvesting cells with 1x SDS sample buffer, immediately followed by denaturing samples in boiling water for 15 min prior to separation on an SDS-PAGE.

Western blotting was carried out using a standard protocol. Briefly, the PVDF membrane was first incubated with 5% non-fat milk in 1 x TBS buffer containing 50 mM Tris-HCl (pH7.4), 150 mM NaCl plus 0.1% Tween 20 at room temperature for 1 h. The membrane was then incubated with a primary antibody diluted in the primary antibody dilution buffer containing 1 x TBS, 0.05% Tween 20, 0.02% NaN<sub>3</sub> and 5% BSA at room temperature for 1 h, followed by three washes with 1 x TBST buffer containing 1 x TBS and 0.1% Tween 20 for totally 30 min. The membrane was further incubated with a secondary antibody in 1 x TBST at room temperature for 1 h prior to washing with 1x TBST for 30 min. The protein signal was visualized by chemiluminescence using Immobilon Western system (Millipore). β-actin was used as a loading control. Antibodies used include: rabbit anti-Cep85 (26314-1-AP, Proteintech; 1:1,000), mouse anti-Nek2A (BD Biosciences; 1:1,000), mouse anti-cyclin B1 (GNS-1, BD Biosciences; 1:1,000), mouse anti-β-actin (AC15, Sigma-Aldrich; 1:5,000), mouse anti-FLAG M2 antibody (F1804, Sigma-Aldrich; 1:500), mouse anti-HA (SC-7329, Santa Cruz Biotechnology; 1:1,000), mouse anti-Plk1 (ab 17057, Abcam; 1:1,000), rabbit anti-Cep85pT392 (this study; 1:2,000), rabbit anti-pericentrin (ab4448, Abcam; 1:2,000) mouse anti-Myc (SC-40, Santa Cruz Biotechnology; 1:1,000), mouse anti-6xHis (66005-1-Ig, Proteintech; 1:5,000), and rabbit anti-GFP (Ab290; Abcam; 1:5,000).

### **Protein purification.**

Recombinant GST fusion Cep85 proteins were expressed in *E. coli* by transforming pGEX-4T-1-Cep85 constructs into BL21 (DE3) bacteria, induced with 1 mM of IPTG for 3h at 37°C, and affinity purified using glutathione-agarose resin (Thermo Scientific). Recombinant His-tagged proteins were expressed in Sf9 insect cells using pFastBac-HTA carrying respective inserts as a donor plasmid according to the instruction manual of the Bac-To-Bac Baculovirus Expression System (Invitrogen) and affinity purified with Protino Ni-NTA Agarose (Macherey-Nagel).

### **In vitro binding assays.**

The recombinant GST (~3 µg per reaction) or GST-fused Cep85 proteins (~3 µg per reaction) on

beads were incubated with recombinant His-Plk1 (1.0 µg per reaction) or with HEK293T cell lysates that overexpressing respective HA- or FLAG-tagged proteins (4 µg plasmid per 35 mm petri dish) in the binding buffer containing 50 mM Tris-HCl pH 7.4, 150 mM NaCl, 1 mM EDTA and 0.2% NP-40, supplemented with 10 µg/ml pepstatin A, 10 µg/ml leupeptin and 1 mM PMSF in a total reaction volume of 500 µl on a rocking platform for 4 h at 4 °C. Beads were washed three times using the binding buffer followed by boiling in 1x SDS sample buffer. Input and bound proteins were analyzed by immunoblotting.

### **In vitro kinase assays**

The in vitro kinase assays were performed as described previously(Chen et al., 2015) with some modifications as follows:

To identify kinase that can phosphorylate Cep85 in vitro, either immunoprecipitated FLAG-Cep85 or recombinant GST-Cep85 was used as a substrate for immunoprecipitated kinases. To immunoprecipitate FLAG-Cep85 and kinases, 4 µg of the respective plasmid was transfected into HEK293T cells in a 35 mm petri dish to express protein for 24 h prior to immunoprecipitation as described above. For using GST-Cep85 as a substrate, recombinant GST (~3 µg per reaction) and GST-Cep85 (~3 µg per reaction) proteins on beads were either directly incubated with immunoprecipitated HA-tagged kinases that were overexpressed in HEK293T cells or preincubated with tagged Nek2A proteins overexpressed in HEK 293T cells prior to further incubation with immunoprecipitated kinases for the in vitro kinase reaction. To pre-incubate GST-Cep85 protein with proteins overexpressed in HEK293T cells, the in vitro binding assays described above were used. The reaction in a kinase reaction buffer containing 20 mM Tris-HCl pH 7.5, 50 mM KCl, 10 mM MgCl<sub>2</sub>, 1 mM DTT, and 8 µM ATP with or without 10 µCi [ $\gamma$ -<sup>32</sup>P]ATP (Amersham) was carried out in a total reaction volume of 40 µl on a rocking platform for 4 h at 30 °C. The reaction was stopped by supplementing with 10 µl of 5 x SDS sample buffer prior to separation on a SDS-PAGE followed by Coomassie Brilliant Blue (CBB) stain, Western blot analysis and autoradiography if applicable.

To compare the binding affinity of Nek2A proteins to either Cep85 protein or phosphorylated Cep85 protein by Plk1, pre-binding of Nek2A proteins to GST or GST-Cep85 proteins on beads and the kinase reaction in the presence or absence of ATP were performed as described above. After reaction, beads were washed three times using the reaction buffer without ATP followed by heating in 50 µl of 1x SDS sample buffer prior to analysis.

### **Measurement and statistics**

The fluorescent intensity of immunostained proteins at centrosome and the distance of centrosomes were measured using ZEN 2010 software (Carl Zeiss, Germany) and ImageJ according to the methods previously described(Mardin et al., 2010). The intensities of Western blot bands and autoradiograph bands were quantified by densitometry and normalized to the control. Data were processed with GraphPad Prism 6 and Statistical significance was determined by unpaired two-tailed t-tests.

### **Supplemental References.**

Sancak, Y., Peterson, T.R., Shaul, Y.D., Lindquist, R.A., Thoreen, C.C., Bar-Peled, L., and Sabatini, D.M. (2008). The Rag GTPases bind raptor and mediate amino acid signaling to mTORC1. *Science* 320, 1496-1501.